ER79-4032

SOLAR POWER SATELLITE (SPS) PILOT BEAM & COMMUNICATION LINK SUBSYSTEM INVESTIGATION STUDY - PHASE I

Prepared For

NATIONAL AERONAUTICS AND SPACE ADMINISTRATION
GEORGE C. MARSHALL SPACE FLIGHT CENTER
HUNTSVILLE, ALABAMA 35812

Under Contract NAS8-33157
DCN 1-8-PP-00800

(NASA-CR-161161) SOLAR POWER SATELLITE (SPS) PILOT BEAM AND COMMUNICATION LINK SUBSYSTEM INVESTIGATION STUDY, PHASE 1 Final Report (Raytheon Co.) 85 p HC A05/MF A01 CSCL 22B G3/15
N79-17896
Unclas
16087

MAR 1979
RECEIVED
NASA STI FACILITY
ACCESS DEPT.

Prepared By

RAYTHEON COMPANY
Equipment Division
Advanced Development Laboratory
Wayland, Massachusetts 01778

31 January 1979

ER79-4032

SOLAR POWER SATELLITE (SPS) PILOT BEAM & COMMUNICATION LINK SUBSYSTEM INVESTIGATION STUDY - PHASE I

Prepared For

NATIONAL AERONAUTICS AND SPACE ADMINISTRATION
GEORGE C. MARSHALL SPACE FLIGHT CENTER
HUNTSVILLE, ALABAMA 35812

Under Contract NAS8-33157
DCN 1-8-PP-00800

Prepared By

RAYTHEON COMPANY
Equipment Division
Advanced Development Laboratory
Wayland, Massachusetts 01778

31 January 1979

ABSTRACT

A study of the Pilot Beam and Communication Subsystem aspects with primary attention paid to ionospheric and RFI/EMI issues was conducted by Raytheon as part of the NASA/MSFC continuing studies on the feasibility of power transmission from geosynchronous orbit.

A preliminary engineering model of the ionospheric interactions with the pilot beam was established and used to demonstrate that the dual frequency baseline pilot beam system might not be viable in the presence of an unstable transmission path. Alternate approaches to remove this difficulty were proposed and are described in detail. Analysis of the effects of ionospheric fluctuations on the microwave power beam show that although ionospheric fluctuations will not significantly degrade beam pointing or raise the sidelobe levels, the ionospheric fluctuations will reduce transmission efficiency by upwards of 25%. Mitigating strategies to substantially reduce this effect were proposed.

Based on the Klystron noise spectrum the pilot beam transmitter power was determined as a function of frequency offset from the power beam carrier frequency. The RFI from the pilot beam, on the ground and at geosynchronous orbit is shown. Further, the noise levels on the earth's surface due to the SPS are presented as a function of frequency and the number of SPS systems.

Analysis of the communication subsystem indicated that a standard telemetry line of 1.544 MB/s would satisfy both voice and data link requirements. Additional links would be required for TV and radio transmissions which are used primarily for entertainment. RFI and EMI from the communication subsystem does not appear to be a significant issue.

Finally, recommendations are presented for additional investigations of critical issues identified during the Pilot Beam and Communication Subsystem study.

FOREWORD

This is the Technical Report for Phase I of the Solar Power Satellite (SPS) Pilot Beam & Communication Link Subsystem Investigation Study. The study was performed for NASA Marshall Space Flight Center. The study was carried out under the overall management cognizance of O. E. Maynard.

The Pilot Beam - Ionospheric Interaction Task was undertaken by A. H. Katz and Dr. M. Grossi. The Pilot Beam Sizing and RFI and Communications Subsystem Analysis was undertaken by J. Howell and W. Bickford respectively.

This work supplements previous Raytheon investigations under NASA contracts which include the Lewis study CR-134886, December 1975 (Microwave Power Transmission System Studies, Vol. II) and the MSFC study, under subcontract ECON-0003, March 1977 (Space-Based Solar Power Conversion & Delivery System Study, Vol. III).

TABLE OF CONTENTS

Section		Page
1.0	INTRODUCTION	1-1
2.0	EXECUTIVE SUMMARY	2-1
2.1	STUDY BACKGROUND	2-1
2.2	MSFC PILOT BEAM BASELINE SYSTEM	2-2
2.3	SUMMARY OF STUDY	2-3
2.3.1	Pilot Beam- Ionospheric Interactions	2-3
2.3.2	Pilot Beam Sizing and RFI	2-5
2.3.3	Communication System	2-6
3.0	PILOT BEAM: IONOSPHERIC INTERACTIONS	3-1
3.1	INTRODUCTION	3-1
3.2	IONOSPHERIC MODEL	3-2
3.2.1	Requirements For The Ionospheric Model	3-2
3.2.2	Engineering Model Of The Ionosphere And Of The Ionospheric Interactions	3-3
3.2.3	Observational Data Base	3-5
3.2.4	Initial Estimates Of Phase Errors Due To Ionospheric Interactions	3-9
3.3	MULTI-FREQUENCY PILOT BEAM SYSTEM AND THE IONOSPHERE	3-11
3.3.1	Statement Of The Problem	3-11
3.3.2	Ionospheric Effects On The Dual Frequency Pilot Beam Baseline	3-12
3.3.3	Possible Approaches For The Correction Of Ionospheric Induced Ambiguities In The SPS Pilot Beam System	3-14
3.3.3.1	Introduction	3-14
3.3.3.2	Approach No. 1	3-15
3.3.3.3	Approach No. 2	3-23
3.3.3.4	Approach No. 3	3-26
3.3.3.5	Conclusions	3-27
3.4	PHASE ERRORS DUE TO IONOSPHERIC FLUCTUATIONS	3-28
3.4.1	Statement Of The Problem	3-28
3.4.2	Effects Of Phase Errors On The SPS Power Beam	3-31

TABLE OF CONTENTS

Section		Page
3.4.2.1	Beam Efficiency	3-33
3.4.2.2	Beam Pointing Accuracy	3-35
3.4.2.3	Sidelobe Level	3-35
3.4.3	Mitigating Strategies	3-38
3.4.3.1	Spatial Diversity	3-38
3.4.3.2	Temporal Diversity	3-40
3.4.3.3	Frequency Diversity	3-40
3.5	RECOMMENDATIONS FOR PHASE III	3-42
3.6	REFERENCES	3-44
4.0	PILOT BEAM SIZING & RFI	4-1
4.1	INTRODUCTION	4-1
4.2	PILOT BEAM SIZING	4-1
4.2.1	Interference Levels	4-1
4.2.2	Mutual Coupling	4-3
4.2.3	Suppression of Klystron Leakage	4-8
4.2.4	Pilot Beam Transmitter Power	4-8
4.3	SPS RFI PROBLEMS	4-8
4.3.1	SPS Noise Levels on the Earth's Surface (Single SPS)	4-8
4.3.2	Power Density From The Pilot Beam	4-11
5.0	COMMUNICATIONS SUBSYSTEM	5-1
5.1	INTRODUCTION	5-1
5.2	COMMUNICATION REQUIREMENTS	5-1
5.2.1	Telemetry (SPS To Ground)	5-1
5.2.2	Command And Control (Ground to SPS)	5-2
5.2.3	Operations (Two-Way Link)	5-2
5.2.4	Entertainment	5-4
5.3	COMMUNICATION SUMMARY	5-4
5.3.1	Digital Communications Summary	5-4
5.3.2	Entertainment Transmission System	5-5
5.3.3	Transmitted Power Required	5-5
5.4	FREQUENCY ALLOCATION AND RFI	5-6
5.5	RECOMMENDATIONS FOR PHASE II	5-6

LIST OF ILLUSTRATIONS

Figure		Page
3.1	Spectral density of the relative fluctuations in plasma density detected during a rocket flight from Brazil (from Basu & Kelley, 1977)	3-6
3.2	The dashed line is a model spectrum used by Costa & Kelley (1976)to characterize the breakup of density gradients in upwelling structures. The solid line is a spectrum used by Basu & Basu (1976a) to typify extended topside irregularities. (From Basu & Kelley, 1977)	3-8
3.3	Frequency dependence of phase-scintillation index, during two 20 sec periods of the pass above Poker Flat, 29 May 1976 compared with an f^{-1} dependence. (from Fremouw et al, 1978)	3-10
3.4	Frequency dependence of phase scintillation index during two 20 sec periods of pass recorded at Ancon on 16 Dec. 1976, compared with an f^{-1} dependence arbitrarily passed through the 413 MHz data point. (from Fremouw et al, 1978)	3-10
3.5	Simplified Block Diagram of Approach No. 1	3-16
3.6	Block Diagram of Realizable System for Approach No. 1	3-20
3.7	Block Diagram of Approach No. 2	3-24
3.8	Schematic Representation of Power Beam & Pilot Beam	3-29
3.9	Expanded view of ionospheric interaction region for both pilot beam and power beam	3-30
3.10	Expanded view of ionospheric interaction region for pilot beam	3-32
3.11	Reduction in Beam efficiency ϕ vs rms phase error	3-34
3.12	RMS Beam pointing angle vs rms phase error	3-36
3.13	SPS Antenna gain vs angle from boresight	3-37
4.1	Interference sources at SPS subarray	4-2
4.2	Total interference vs pilot beam frequency	4-5
4.3	Mutual Coupling Calculations	4-6

LIST OF ILLUSTRATIONS (Cont.)

Figure		Page
4.4	Coupling Coefficients	4-7
4.5	Cancellation of Transmit Leakage Using a Chebyschev Filter	4-9
4.6	Pilot Transmitter Sizing	4-10
4.7	Noise on Earth From SPS Array	4-12
4.8	SPS Noise Level at Earth (Single SPS)	4-13
4.9	Harmonic Output of Converters in dB below fundamental (Radar Handbook, Skolnik, p. 29-G)	4-14
4.10	Power Density in vicinity of pilot transmitter (Range = 10 KM)	4-15
4.11	RFI in Orbit due to Multiple Pilot Transmitters	4-17
5.1	Communications System Network	5-7

- - - - -

LIST OF TABLES

Table		Page
2.1	MSFC Pilot Beam Baseline System (Oct. 1978)	2-2
2.2	Summary of Phase I Pilot Beam Study	2-4
3.1	Number of Ambiguities (N) vs Δf	3-13
3.2	Mitigating Strategies to Reduce Ionospheric Induced Phase Fluctuation	3-39
4.1	Pilot Transmitter Sizing Interference Levels	4-4

1.0 INTRODUCTION

The objective of the Solar Power Satellite (SPS) Pilot Beam and Communication Subsystem Study is to investigate pilot beam and communication link subsystem aspects with attention paid to environmental issues such as atmospheric and RFI/EMI problems. Phase I, as described by this report, provides an overall assessment of the technical issues, provides preliminary results, and identifies the technical risks where further in-depth analysis is required. Options for Phase II will concentrate on a selected set of these technical risk areas and will provide recommendations for experimental verification of those areas which have a particularly high technical risk.

The results of this study will provide inputs to the environmental assessment of RFI/EMI issues currently underway by DOE/ITS. The results will also be of use in the planning for the GBER (Ground Based Experimental Research) Program as it is related to the pilot beam system. Raytheon is participating in DOE's SPS Environmental Assessment program and as such will facilitate the transfer of the results of this program to the DOE program. In fact, our participation in this study and the DOE program has resulted in a synergistic relationship where a strong connection between system requirements and specifications with ionospheric physics has been made.

The Phase I program has been divided into three tasks which are highlighted below:

Task 1. Pilot Beam-Ionospheric Effects

The objective of this task is to analyze the potential effects that the ionosphere will have on the pilot beam system. Our approach is to generate an engineering model for the ionosphere and determine its impact on the pilot beam system. Specifically the ionospheric impact on the dual frequency phase control system will be addressed. In addition, a prediction of the ionospherically induced rms phase errors on the pilot beam system and its impact on the performance of the SPS system, including an analysis of mitigating strategies, will be provided.

Task 2. Pilot Beam-Sizing & RFI

This analysis will determine the power aperture product of the pilot beam transmitter as required by the phase control system. This data will be used to assess the RFI originating from the pilot beam system observed on the ground as well as observed at geosynchronous orbit. In addition the noise and interference, measured on the earth's surface, from the Klystron (SPS microwave generating tube) will be determined.

Task 3. Communication Study

During Phase I, the communication systems required by SPS are to be delineated. This will include, for example, links from the rectenna to the SPS and links from the launch vehicles (HLLV, POTV, COTV) to the logistics base at LEO. However, during Phase I, only the link between the SPS and the rectenna will be analyzed in depth. This is the primary command and contral link. The links will be analyzed for 30, 60, and 120 SPS configurations and will include redundant system. The objective of the Phase I effort is to identify the new radiators that will occur because of the SPS system and to size the radiation for the command and control communication links between the rectenna and the SPS.

Section 2.0 of this report contains an Executive summary. Details of the Pilot Beam Ionospheric Interactions, Pilot Beam Sizing & RFI, and Communication tasks can be found in Sections 3.0, 4.0, and 5.0 respectively. Recommendations for Phase II of this effort are contained in Section 6.0.

2.0 EXECUTIVE SUMMARY

2.1 STUDY BACKGROUND

Several initial studies of the adverse effects conceivably associated with the high power SPS downcoming microwave beam have identified the following principal risk areas:

1. Impact on the medium crossed by SPS - This includes the environmental effects of the launch vehicles, the interaction between the power beam and the earth's atmosphere (both ionized and neutral), and the distribution of RF energy at and near the earth's surface.
2. Biological effects on the population and on other living beings - The minimization of these effects has dictated the adoption of a pilot beam that keeps the high power microwave irradiation strictly limited to the rectenna area on the earth's surface.
3. The Radio Frequency Interference (RFI) produced at the fundamental frequency of the power beam (and at the other frequency components of the necessarily finite spectral width around it) and at harmonic frequencies - Users potentially perturbed by this interference are the electromagnetic systems that may operate in the general proximity of the SPS beam, such as communication/command-control systems, navigation/positioning systems, direction finders, radars, etc.

The overall problem, however, has several aspects that have not been covered by the previous studies and that come from a cross-coupling of the items above. For instance, RFI is not only produced by the power beam transmitter but also by the pilot beam transmitters and by the transmitter of the communication/command-control link between the ground and SPS.

In addition, the impact of the power beam on the geophysical medium (the issue mentioned in Item 1)makes it difficult to transmit to SPS, through the same medium, a pilot beam with the coherence of its wave front preserved well enough to provide a reliable positional reference.

This effort aims at the identification of these kinds of issues that require further study and at the formulation of mitigating approaches suitable for the problem areas, so that tradeoff comparisons among these potential solutions can be conducted and an optimum approach chosen for each one of them.

2.2 MSFC PILOT BEAM BASELINE SYSTEM

For the Pilot Beam, a baseline system (dated as of October 1978) and recommendations for investigating this baseline were established. The baseline and items studied in this report are listed in Table 2.1.

Table 2.1. MSFC Pilot Beam Baseline System (Oct. 1978)

Baseline	Recommendations For Study
1. Single transmitter, two frequency (2.35 & 2.55 GHz, ± Δf centered at 2.45 GHz).	1. Parametric data on effect of varying Δf vis-a-vis power aperture product for pilot beam transmitter. Effects of ionosphere as a function of Δf is also studied.
2. Conjugating system on GEO is Rockwell (RF at 2.45 GHz).	2. This is a point of departure from the JSC (Lincom) system which implements conjugation at IF. This point of departure is to be explored and impact assessed in Phase II of this program.
3. Whole subarray (10 x 10 m) is receiver for pilot system.	3. Parameter study on reducing size of pilot beam receiver to at least single (Klystron) tube which is 1/36 of subarray.
4. Noise spectrum of tube (Klystron)	4. We are to use available information and provide our own where appropriate.
5. Phase error budget	5. From Rockwell study and is 13° rms independent of propagation.
6. Time constant of conjugating system.	6. Current concept is as fast as possible with 10 μsec as a nominal value.
7. Diode phase shifter and monopulse	7. How accurate is digital phase shifter and how does it relate to monopulse?
8. Redundancy	

2.3 SUMMARY OF STUDY

Table 2.2 is an overall summary of the study. There are three major areas listed and the results are briefly summarized below.

2.3.1 PILOT BEAM-IONOSPHERIC INTERACTIONS

Two areas were identified. The first is an analysis of the effect of the steady state (unperturbed) ionosphere (bias) on the baseline pilot beam system. (The baseline system used two frequencies separated by $\Delta F = 100$ MHz from the carrier.) This study established that this dual frequency system might not be viable in the presence of an unstable transmission path. However, several alternate approaches for bias removal have been identified and are described in this report. These approaches, essentially based on comparing phase paths at three frequencies, must be investigated in greater detail both with respect to ionospheric interactions and their impact on the design of the baseline SPS system. However, there appear to be 3-frequency solutions which will remove the ionospheric effects on the pilot beam system from the category of potential program stopper to one which only requires some further technical investigations.

The second area was an analysis of rms phase fluctuations on the pilot beam signal due to ionospheric fluctuations and their impact on system performance. The results indicate that rms phase errors upwards of 40 degrees are possible (exclusive of ionospheric heating effects due to the SPS power beam). This phase error should not significantly degrade pointing accuracy of the power beam or significantly increase sidelobe levels of the SPS power beam. However, unless the magnitude of the ionospheric induced phase errors is reduced, these phase errors could degrade system efficiencies of as much as 25% and further, since the ionospheric effects are time varying, result in an unacceptable time-varying SPS power output delivered to the ground based power grid.

Several mitigating strategies, to reduce the rms phase error from ionospheric fluctuations had been proposed. These strategies are viable only if the removal of the bias is performed first as done with the alternate approaches for the pilot beam system described in this report. The major uncertainty that still remains is the effects of the ionospheric heating due to the SPS power beam and the occurrence statistics, in time and space, of the ionospheric fluctuations. The

TABLE 2.2. SUMMARY OF PHASE I PILOT BEAM STUDY

AREA	RESULTS OF STUDY	RECOMMENDATIONS
Ionospheric Interactions	Baseline concept not valid in presence of unstable transmission path. Alternate approaches recommended. Mitigating strategy to reduce phase fluctuations presented.	Investigate alternate approaches vis-a-vis ionospheric interactions. Investigate mitigating strategies to reduce RMS phase error. Investigate impact of time fluctuations of power on interface to power grid. Develop experimental program for GBER (power beam heating).
Pilot Beam System	Pilot System sized. Levels of RFI from pilot beam provided. (Depends on freq. separation from carrier and size of subarray).	Utilize approach which maximizes Δf. This might conflict with ionospheric effects and should be studied. Study implementation of alternate approaches described above. RF vs IF phase conjugation still requires study.
Communication System	Requirement established. Off-the-shelf standard comm. gear. Low Power - 25 mW data links, 1 W TV links	Study decentralized vs centralized concepts (not a high priority item).

results of this study should be used to form the basis for experiments that should be conducted during the GBER and which will provide the information necessary to design and implement the appropriate phase control system.

2.3.2 PILOT BEAM SIZING AND RFI

In this task the pilot beam transmitted power as a function of frequency separation from the carrier (2.45 GHz) and was calculated. In addition, SPS RFI problems and RFI from the pilot beam were addressed.

The pilot beam sizing depends on interference levels from thermal noise, Klystron noise leakage, and Klystron noise from other Klystrons through mutual coupling. Calculations for these three interference levels are provided as a function of frequency separation of the pilot tone from the carrier. At frequency spacings of 100 MHz, the pilot beam requires 0.1 W transmitted power for a 10 m pilot beam antenna. For 5 MHz tone separation, a 45 kW pilot transmitter is required. This is due to the increase interference from coupled Klystron noise which occurs below 25 MHz pilot tone separation. The transmitter power is increased by a factor of 25 if a single Klystron replaces the 10 x 10 m subarray as the smallest element which is phase controlled.

Noise levels from a single SPS at the Earth's surface are shown as a function of frequency from 1450 to 3450 MHz. For separation greater than 25 MHz from the carrier, the noise levels vary from -280 to -24 $dBW/m^2/Hz$ while for close in noise levels (within 35 MHz), the level is approximately -187 $dBW/m^2/Hz$. For 60 SPS systems the power density increases by 18 dB.

Power density in the vicinity of the pilot transmitter (range = 10 km) for pilot tone separation greater than 25 MHz is -100 dBW/m^2 for the isotropic sidelobes and -55 dBW/m^2 for the peak of the beam. For pilot beam separation of 5 MHz, the power density is -45 dBW/m^2 for sidelobes and 0 dBW/m^2 at the peak of the beam.

Multiple pilot transmitters on the earth create an interference problem at a given SPS system. Only one pilot beam is actually aimed at that SPS but the sidelobes of the other pilot beams are an interference source. The 100 SPS systems can be spread over a 60° equatorial arc with only one SPS in a given

pilot beam. If the pilot beam peak sidelobes are less than 20 dB, all the interference pilot beams cannot create as much power at a particular SPS as its dedicated pilot beam.

Recommendations for Phase II of the pilot beam are to study the impact the alternate approaches and mitigating strategies required because of ionospheric interactions,as summarized in Section 2.3.2 and described in Section 3,have on the design and implementation of the pilot beam system.

2.3.3 COMMUNICATION SYSTEM

The communication requirements were established and specified a 1.544 Mb/s voice and data link. This voice and data link includes Command and Control functions (uplink path), Telemetry of data from SPS to Ground Control Station, and station operations (two-way link). Entertainment is a separate TV and radio link. The 1.544 Mb/s data link is standard in many telephone applications. The use of a standard communications link means that off-the-shelf equipment is available for both transmissions and encryption of the data. The 1.544 Mb/s channel consists of 24 channels each with 64 kb/s data rate and includes 8 spare channels. A transmitted power of 25 mW would satisfy the needs for the 1.544 Mb/s voice and data link. One Watt would be required for the color TV entertainment link. These calculations assumed 8 GHz frequency band, 20 meter ground antenna, 3 meter spacecraft antenna, and an 8 dB system noise factor.

The communication requirements and resultant sizing of the Communication system have been provided. The study has demonstrated that the SPS communication requirements are relatively modest and will not create a significant RFI problem. There remains, however, the question of how to distribute the information to the space stations. For example, the Central Control talks directly to the Rectenna Control station and the Rectenna station talks to the SPS. Alternatively, a centralized network is used and leads to an interesting antenna complex if all earth-space links terminate at a central site.

As a result of this study, we recommend that during the Phase II program the issue of centralized vs centralized communication network be explored. However, as we feel that this is a low priority effort and could, without impacting on the SPS development (at least as we view it), be delayed to a later time.

3.0 PILOT BEAM-IONOSPHERIC INTERACTIONS

3.1 INTRODUCTION

The specific objectives of this task are to analyze the ionospheric interactions and the pilot beam system with respect to:

a. Effects of the unperturbed ionosphere (bias) on the performance of the pilot beam system with specific attention to the dual frequency (baseline) phase control system.

   The dual frequency system transmits two pilot tones from the ground at $f_o \pm \Delta f$ ($f_o = 2.45$ GHz). The basic assumption made is that an average of the phase at $f_o \pm \Delta f$ ($\Delta f = 100$ MHz) will duplicate the phase if a single pilot tone at f_o was utilized. This assumption will be analyzed in detail in Section 3.2.

b. Effects of phase errors on power beam due to phase and amplitude fluctuations arising from inhomogeneities in the ionosphere.

   Phase errors caused by the ionosphere will be translated into a reduction in power transmission efficiencies, pointing errors of the SPS power beam, and increased sidelobe levels. This study will provide the range of ionospheric induced phase errors to be expected and also indicate the impact of these phase errors on the SPS system performance. Section 3.3 will contain this analysis.

It is worthwhile to reemphasize the differences between the two objectives. Analysis directed toward the first objective depends on an ionospheric model which is well understood (an extensive data base is available for analysis) and the ionospheric effects are 0th order. By 0th order, we mean that the effects are independent of space and time within the context of the operation of the pilot beam system (i.e., the time constant of the pilot beam system is short compared to the ionospheric time and spatial variations). The analysis directed toward the second objective depends on an ionospheric model which is somewhat speculative (a minimal data base is available, particularly with respect to operational characteristics of the pilot beam system and in addition the ionospheric effects of SPS power beam heating are not yet known) and the ionospheric effects are first and second order. By this we mean that the effects are highly space and time dependent and that the distribution of the events in time is not known.

Section 3.2 will describe the ionospheric model and provide initial estimates of the phase errors due to ionospheric interaction. Section 3.3 will analyze the effects of the ionosphere on the dual frequency (baseline) phase control system and provide possible approaches for the correction of ionospheric induced ambiguities in the SPS pilot beam system. Section 3.4 will describe the phase errors due to ionospheric fluctuations, their effects on the SPS power beam and potential mitigating strategies. Recommendations for the Phase II study with respect to ionospheric interaction can be found in Section 6.0.

3.2 IONOSPHERIC MODEL

3.2.1 REQUIREMENTS FOR THE IONOSPHERIC MODEL

The interaction of the pilot beam with the ionosphere must be studied in its several aspects:

a. non-stochastic phase perturbations induced in the beam by naturally occurring ionospheric large-scale features (such as wedges and slabs) affecting differently (if their spatial scale permits it) the radio paths that go from the ground terminal of the pilot beam to different points of the SPS array;

b. stochastic phase perturbations induced in the pilot beam by naturally occurring ionospheric turbulence;

c. phase perturbations induced in the pilot beam by artificial ionospheric irregularities caused by the SPS, downcoming, power beam;

d. scattering of the pilot beam by the natural and artificial ionospheric perturbations mentioned in the previous points and estimation of the interference thus produced by the pilot beam against other users of the same frequency band.

Items a, b, and c above potentially affect the ability of the power beam to function as an accurate pointer of the downcoming SPS power beam, thus impacting on the environmental hazard connected with SPS operations. Item d is of lesser importance and falls in the area of radio-frequency interference caused in part by the non-linear interactions of the SPS power beam with the ionosphere.

In order to evaluate in a definitive way all the effects above, what is needed is a comprehensive model of the interactions of the SPS power beam with the ionosphere. However, this model does not exist yet, and the situation will not change in this respect for several years. Therefore, in the time interval between now and the date at which the DOE Environmental Impact Program will complete its work, it is necessary and expedient to generate an interim model, a sort of "Engineering Model", based on present knowledge of the ionosphere and of the interactions with this medium of the SPS power beam and of the pilot beam itself.

In the following sections, we illustrate the work that we have performed during Phase I toward the generation of this Engineering Model. This work is still in progress and we plan to complete it during Phase II.

3.2.2 ENGINEERING MODEL OF THE IONOSPHERE AND OF THE IONOSPHERIC INTERACTIONS

The Engineering Model that we have started generating during Phase I consists of the following basic parts:

Part No. 1 - Three-dimensional model of the smooth ionosphere (exclusive of turbulence and of localized features but inclusive of day/night transitions);

Part No. 2 - Model of ionospheric wedge suitable for addition to the model of the smooth ionosphere of Part 1;

Part No. 3 - Model of naturally-occurring ionospheric turbulence;

Part No. 4 - Model of ionospheric turbulence artificially induced by the SPS power beam.

Part No. 1 Model is already available to us in the form of a FORTRAN software program and makes it possible to compute phase path lengths, group path lengths, total electron content (TEC), etc., between ground terminals and spaceborne terminals such as SPS in synchronous orbit. This model is based on the formulation contained in Report AFCRL-TR-73-0657 (SAMSO-TR-73-252) dated July 1973, known as the Bent ionospheric model. We have chosen this formulation because it is one of the most accurate ionospheric models available from the standpoint of computing the e.m. properties of ground-to-space trans-ionospheric paths, among which the TEC, the "ionospheric bias," etc. The

program can generate ionospheric data on a world-wide basis for any past or future date. For a given set of inputs, consisting of ground station position, satellite position and time information, the profile of the electron density along the line of sight is computed first and then the program computes among other things, range, range rate, angular refraction, and so on. The model has the additional capability of improving its predictions by updating them with actual ionospheric observations. Considerable tests in the past have proved this model highly successful.

The computation of the quantities of direct interest to the SPS pilot beam study does not require therefore the addition of a ray-tracing program inasmuch as these quantities are provided directly by the model software, based on a straight-line approximation to a ray quite justifiable at our frequency.

One of the most important uses of this model is to verify, in case of the adoption of a multi-frequency pilot beam system (for removal of ionospheric bias), how far apart the various carriers can be placed without incurring in the problem of 2π ambiguity in relative phase measurement in ground-to-SPS links.

Concerning Part No. 2 of the Engineering Model, we are constructing an analytical model of an ionospheric wedge simulated as the side ramp of a three-dimensional gaussoid, characterized by variable steepness, and therefore capable of modeling gradients of different value that may intersect the pilot beam. This model will make it possible to analyze in a quantitative way (based on geometric optics) the realism of the pessimistic assumption that a single-frequency pilot beam system could not possibly work because of the different "bias" seen by the various paths from the ground to the several measuring points of the SPS array.

Concerning Part No. 3, we are working at the refractive scattering approach (Crain and Booker, 1978), the only formulation that appears to provide analytical results that are close the large phase perturbations observed at microwave frequencies in transionospheric paths involving equatorial, tropical and auroral regions. We plan to computerize this approach and to construct the related model during Phase II of the pilot beam study program.

Finally, concerning Part No. 4, we have reviewed the theoretical formulations that were developed by Raytheon in 1975 on the occasion of NASA Study Contract NAS 3-17835 (see the chapter "Self-focusing Instabilities", Appendix B,

Raytheon Report ER75-4368, dated December 1975). On the basis of these formulations, we plan to arrive during Phase II at a model that, however crude, will make it possible to compute numerically the pilot beam phase perturbations due to artificial ionospheric modification induced by the downcoming SPS power beam.

3.2.3 OBSERVATIONAL DATA BASE

The unexpectedly large scintillation indices that have been observed since the early '70s in space-to-ground microwave links that go through the night-time F-region of the ionosphere at equatorial, tropical, and auroral latitudes have prompted considerable interest in generating an adequate data base for this phenomenon. These occurrences of ionospheric turbulence directly affect the phase stability of a radio link such as our Pilot Beam System and are therefore of immediate concern to our study. Part No. 3 of the Engineering Model mentioned in Section 3.2.2 must in fact be in good agreement with this experimental evidence. Sources of observational data that we have reviewed during Phase I study include papers and reports by several authors at AFGL, SRI International, COMSAT Labs, etc.

The review paper by Basu and Kelley (1977) is particularly useful to our undertakings because it summarizes the present understanding of a large category of irregularities, the equatorial ones. These are usually known as Spread-F occurrences and have been studied with in-situ rocket soundings, satellite observations, and radar measurements.

Examples of rocket results are given in Figure 3.1. These were obtained by launching a Javelin 8-63 rocket from Natal, Brazil. In the figure the unit in the y-axis is $\frac{\delta n}{n} / \sqrt{km^{-1}}$ while the x-axis covers wave numbers(*) from approximately 10^{-1} Km^{-1} (spatial wavelength 62.8 Km) to approximately 300 Km^{-1} (spatial wavelength 20.73 m). The results above apply to the bottom-side ionosphere (see in the figure the height reached by the rocket).

By applying the thin screen scattering theory (Costa and Kelley, 1976 and 1977), the mean square phase fluctuation Φ_o^2 can be computed as follows:

$$\Phi_o^2 = \frac{\sqrt{2}}{2} \pi (r_e \lambda) \frac{\alpha}{\beta} (L \sec \theta) \frac{(\delta n)^2}{k_o}$$

(*) At variance with spectroscopy and electromagnetism literature (where wave number = $\frac{1}{\lambda}$, or the number of wavelengths in the unit length) authors of scintillation literature call wave number the quantity $\frac{2\pi}{\lambda}$ that in electromagnetic theory is called the phase constant.

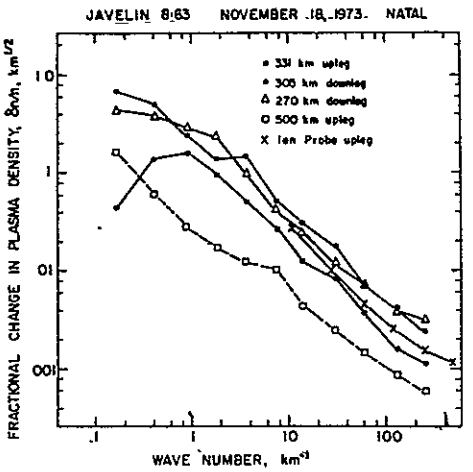

Figure 3.1. Spectral density of the relative fluctuations in plasma density detected during a rocket flight from Brazil (from Basu and Kelley, 1977)

where for equatorial observations:

$$\frac{\alpha}{\beta} \cong 1$$

$$\sec\theta \cong 1$$

$$L = 2 \times 10^4 \text{ m}$$

$$k_o = 1 \text{ Km}^{-1} = 10^{-3} \text{ m}^{-1}.$$

At our frequency of 2.45 GHz ($\lambda = 0.12245$ m), by recalling that the classical radius of the electron is $r_e = 2.818 \times 10^{-15}$ m, we have:

$$\Phi_o^2 = 5.244 \times 10^{-24} (\delta n)^2 \text{ and } \Phi_o = 2.29 \times 10^{-12} (\delta n)$$

From Figure 3.1, by integrating the effect of all the wave numbers larger than k_o, we have:

$$\frac{\delta n}{n} / \sqrt{\Delta \text{km}^{-1}} = 10^{-2}$$

and

$$\frac{\delta n}{n} \cong 10^{-2} \sqrt{300} = 0.1732$$

ORIGINAL PAGE IS
OF POOR QUALITY

By assuming in the bottom-side ionosphere an average electron density of $n \cong 5 \times 10^{11}$ el/m^3, we have $\delta n = 0.86 \times 10^{11}$ and therefore $\Phi_o \cong 0.2$ rad $\cong 11.3°$.

For the top-side ionosphere at the equator, RPA data on electron density irregularities have been collected by the OGO-6 Satellite (orbital height: 400 to 500 Km) and have been analyzed by Basu et al (1976). By applying the same formula for Φ_o^2 that was deduced from thin screen scattering theory and by noticing that in the case of the upper ionosphere, $L = 2 \times 10^5$ m, $k_o = 0.31$ Km^{-1} = 0.31×10^{-3} m^{-1} and $\delta n \cong 10^{11}$ m^{-3}, we have:

$$\Phi_o \cong 0.724 \text{ rad} \cong 41.2° .$$

We point out that this rms value of phase fluctuation is the integrated effect, at f = 2.45 GHz of all wave numbers from k = 1 Km^{-1} to k = 300 Km^{-1}.

A discrepancy becomes immediately evident if we compare the analytical prediction above with actual experimental data. What happens is that an rms error of an amount close to the above is measured as due to irregularities in a wave number interval much smaller than the one used in computing the rms phase fluctuation indicated above. In order to reconcile this discrepancy, a phenomenological shift along the y-axis of Figure 3.1 can be applied. Basu and Basu (1976) have proposed the curve B and B of Figure 3.2 to typify extended topside irregularities. With this curve by adding the effect of all wave numbers between k = 20 Km^{-1} and 300 Km^{-1} (spatial wavelengths from 20.73 m to 314 m), we obtain:

$$\Phi_o \cong 0.699 \text{ rad} \cong 39.8°$$

for the case of interest here (f = 2.45 GHz, etc.).

Basu and Kelley (1977) have also reviewed the COMSAT data that were collected in transionospheric paths and the Jicamarca backscattering data. They found that the morphology of equatorial ionospheric scintillations constructed with these two data sources is in remarkable agreement with the morphology that they derived from rocket and satellite data.

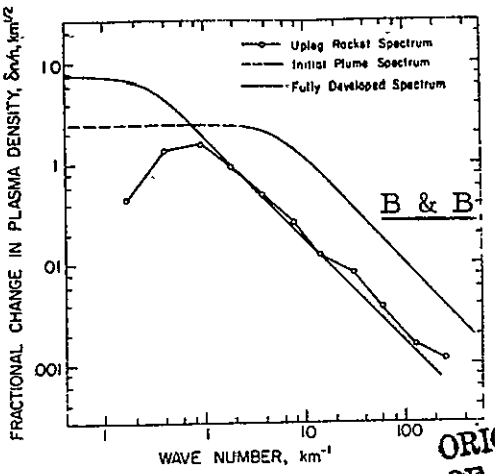

ORIGINAL PAGE IS
OF POOR QUALITY

Figure 3.2. The dashed line is a model spectrum used by Costa and Kelley (1976) to characterize the breakup of density gradients in upwelling structures. The solid line is a spectrum used by Basu and Basu (1976a) to typify extended topside irregularities.
(From Basu and Kelley, 1977)

Another recent important addition to the data base of ionospheric scintillation comes from the DNA-Wideband Satellite Experiment (Fremouw et al, 1978). This coherent multi-frequency transmission (ten spectral lines between VHF and S-Band frequencies) took place from a satellite in a quasi-polar orbit, 1000 Km high and was received on the ground by a network of stations in the equatorial, auroral, and (initially at least) temperate zone. The data generated thus far and the ones that will be generated in the future by this experiment are in principle highly valuable. The raw tapes are sampled at a rate of 500 samples per seconds, although the bulk processing is done at 100 samples/sec. Therefore, because the radio path to the ground sweeps through, at such an altitude of interest as 500 Km with a velocity of 7.72/2 Km/sec = 3.86×10^3 m/sec, the 2 millisecond integration time (correspondent to the 500 samples/sec sampling rate) makes the length of the spatial sample equal to 7.72 m. As a consequence, the shortest spatial wavelength recognizable in the data is about 25 m.

Because we must include among the contributions to phase fluctuations the ones due to irregularities with shorter spatial wavelength, we plan to extrapolate during Phase II activities the DNA-Wideband Satellite observations to those

short wavelengths, (by using for instance the phenomenological model of Basu and Basu, 1976a). This will be done before constructing phase error curves such as the ones depicted in Figures 3.3 and 3.4. Without this corrective approach, Figures 3.3 and 3.4 would give, for the expected phase error at 2.45 GHz, a value of only 30°, less than the value (40°) that at this point in time we believe wise to adopt for our study.

What has not been generated by anybody in the community thus far is the probability distribution curves that establish the percentage of time (y-axis) during which a certain amount of phase error (x-axis) is not exceeded. During Phase II study, we plan to generate, however crude, at least first examples of distribution functions for equatorial, auroral, and temperate regions.

3.2.4 INITIAL ESTIMATES OF PHASE ERRORS DUE TO IONOSPHERIC INTERACTIONS

During Phase I study, we have adopted (admittedly, rather arbitrarily) preliminary estimates for the phase errors induced by the ionosphere in the links of the Pilot Beam System.

We have assumed that the phase errors due to the ionospheric bias and to its spatial variations, when going from an end of the SPS array to the other, are completely removed by the adoption of a multifrequency method for the Pilot Beam System. This can be either the three frequency approach (see Section 3.3.3) that involves only phase measurements, or our proposed approach that uses simultaneously phase delay and group delay measurements. We do believe that this is a realistic assumption because the investigators of the gravitational red-shift rocket probe experiment (Vessot and Levine, 1977) who were working in the S-Band removed any sign of ionospheric bias from their data within 2° or 3° of phase error.

As far as the problem is concerned of the stochastic phase fluctuations, we have adopted the value of 40° for the overall raw phase error at 2.45 GHz, due to natural ionospheric irregularities with spatial wavelength down to 3 m. We do believe that this value is realistic and on the conservative side. As an initial stand, we assume that this value of 40° phase error includes also the phase fluctuations that are expected to be caused by the interaction of the ionosphere with the downcoming SPS power beam.

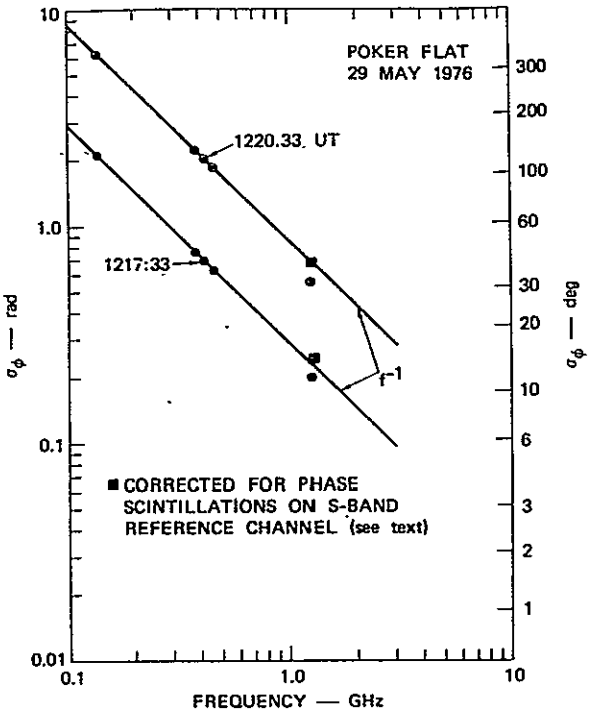

Figure 3.3. Frequency dependence of phase-scintillation index, during two 20 sec periods of the pass above Poker Flat, 29 May 1976 compared with an f^{-1} dependence. (from Fremouw et al, 1978)

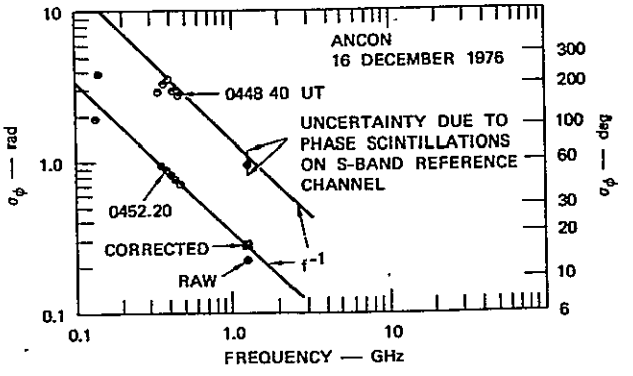

Figure 3.4. Frequency dependence of phase scintillation index during two 20 sec periods of pass recorded at Ancon on 16 Dec. 1976, compared with an f^{-1} dependence arbitarily passed through the 413 MHz data point. (from Fremouw et al, 1978)

3.3 MULTI-FREQUENCY PILOT BEAM SYSTEM AND THE IONOSPHERE

3.3.1 STATEMENT OF THE PROBLEM

The baseline retrodirective pilot beam system utilizes two frequencies spaced 100 MHz above and below the power beam frequency (the power beam frequency is at 2.45 GHz). The pilot beam frequencies are thus allocated far away from the higher noise and interference levels that occur near and at the power beam frequency. This reduces the power aperture product that would be required for the pilot beam system (see Section 4.0). It would appear that only one frequency removed from the carrier would be sufficient. Two frequencies were used in part because it was assumed that this would remove ionospheric biases which would occur if only one frequency removed from the power beam frequency was utilized. This latter assumption is the subject of this section.

The phase measured at the SPS transmitting antenna at $f_1 = f_0 + \Delta f$ and $f_2 = f_0 - \Delta f$ is

$$\varphi_1 = \frac{2\pi f_1 L}{v_\ell} - \frac{40}{f_1}\frac{2\pi}{v_\ell}\int N dl \qquad (1)$$

$$\varphi_2 = \frac{2\pi f_2 L}{v_\ell} - \frac{40}{f_2}\frac{2\pi}{v_\ell}\int N dl \qquad (2)$$

L is the path length from ground based pilot beam to SPS at GEO (37,500 km)

f_0 is the power beam frequency (2.45 GHz)

Δf is pilot beam frequency separation from

v_ℓ is speed of light in free space

$\int N dl$ is the Total Electron Content from pilot beam on ground to SPS at GEO

If one simply averages $\varphi_1 + \varphi_2$ and assumes that $\Delta f^2 << f^{2*}$, it can be shown that $\frac{\varphi_1 + \varphi_2}{2} = \varphi_0$ which is the phase at f_0.

---

* The Gaussian error of 0.2%.

However, this is only correct to modulo 2π. There are, in fact, many 2π differences between f_1 and f_2 over the path length L. Since the phase varies linearly with L, it can easily be corrected by multiplying φ_1 by the ratio f_2/f_1. But if the ionosphere causes modulo 2π phase changes, then the 2π ambiguity cannot be resolved with the current baseline system. Even this would not create difficulties if the ionosphere was spatially and temporally stable. It is anticipated that rms phase fluctuation from ionosphere perturbations could range up to 40 degrees, instantaneous fluctuations would be larger, and this would create serious difficulties with the current baseline configuration which simply averages the phase at f_1 and f_2.

The first step is to show that it is likely that the ionosphere produces a modulo 2π ambiguity in phase between $f_0 + \Delta f$ and $f_0 - \Delta f$ where $\Delta f = 100$ MHz. Of course, one can reduce Δf to a point where the 2π ambiguity does not occur. (Section 3.3.2 will provide a table of the 2π ambiguities versus frequency separation.) This, however, produces another difficulty in that the smaller Δf becomes the closer to the power beam frequency and the larger the noise and RFI levels are with which the pilot beam must compete. The second step is to demonstrate potential solutions which will eliminate the 2π ambiguity and still keep the pilot beam frequencies separated, in frequency space, from the power beam frequency.

3.3.2 IONOSPHERIC EFFECTS ON THE DUAL FREQUENCY BASELINE

In this section, the number of 2π rotations that the ionosphere produces as a function of Δf will be calculated. Multiply Equation (1) for φ_1 by f_2/f_1 and subtract Equation (2) for φ_2 from this and we obtain:

$$\Delta\varphi = \frac{2\pi}{v_\ell} 40 \int N dl \times \left[-\frac{f_2}{f_1^2} \frac{1}{f_2} \right] \tag{3}$$

Substituting into the above equation $f_1 = 2.35$ GHz, $f_2 = 2.55$ GHz, $v_\ell = 3 \times 10^8$ m/sec, $\int N dl = 10^{18}$ el/m^2, we find that $\Delta\varphi = 2\pi \times 9.3$. Thus, for a value of $\int N dl = 10^{18}$ el/m^2 which is a large value but not one which is unusually rare, we find that the ionosphere produces over nine 2π ambiguities. In fact, if the system was designed for an ionosphere of $\int N dl = 10^{19}$ el/m^2 (which is rarely, if ever, exceeded and thus a reasonable design criteria) Δf of 100 MHz produces over nine 2π ambiguities.

Table 3.1 shows the number of 2π ambiguities (N) for a total electron content of 10^{18} and 10^{19} el/m^2 as a function of Δf where $f_1 = f_0 - \Delta f$, $f_2 = f_0 + \Delta f$ and f_0 is 2.45 GHz.

Table 3.1 Number Of Ambiguities (N) vs Δf

Δf MHz	f_1 GHz	f_2 GHz	10^{19} el/m^2 N	10^{18} el/m^2 N	$\int N dl$
100	2.350	2.550	92	9.2	Baseline
50	2.400	2.500	45	4.5	
10	2.440	2.460	8.9	0.89	
5	2.445	2.455	4.4	0.44	
1	2.449	2.451	0.9	0.09	

Table 3.1 shows that to avoid the 2π ambiguities a Δf of 1 MHz would be required. This would resolve the ionospheric ambiguities for all but the most unusual ionosphere. The impact this has on the sizing of the pilot beam transmitter is shown in Section 4. The next section describes procedures for operating the 2π ambiguity and still provide separation from the SPS power beam frequency.

Anticipating the results of the next section a simple calculation will demonstrate the efficacy of the alternate approaches. These approaches basically rely on the utilization of three frequencies for the pilot beam system to calculate the difference of the differences of the phase between the three frequencies (this is essentially determining the second derivative with respect to frequency of the phase as a function of frequency). Using Equation (1) for three frequencies f_1, f_2, and f_3, we obtain $\varphi_1 - \varphi_2$ and $\varphi_3 - \varphi_2$ as:

$$\Delta\varphi_A = \varphi_1 - \varphi_2 = \frac{2\pi}{v_\ell}\left\{(f_1 - f_2)L - \left(\frac{40}{f_1} - \frac{40}{f_2}\right)\int N d\ell\right\}$$

$$\Delta\varphi_B = \varphi_2 - \varphi_3 = \frac{2\pi}{v_\ell}\left\{(f_2 - f_3)L - \left(\frac{40}{f_2} - \frac{40}{f_3}\right)\int N d\ell\right\}$$

if

$$f_1 = f_0 - \Delta f$$

$$f_2 = f_0$$

$$f_3 = f_0 + \Delta f$$

and taking $\Delta\varphi_A - \Delta\varphi_B$, we find

$$\Delta\varphi_A - \Delta\varphi_B = \frac{2\pi}{v_\ell} 40 \int N d\ell \left[- \frac{1}{f_0 - \Delta f} + \frac{1}{f_0 + \Delta f} + \frac{2}{f_0} \right]$$

(note the linear terms in f drop out)
and further

$$\Delta\varphi_A - \Delta\varphi_B = \frac{2\pi}{v_\ell} 40 \int N d\ell \left[\frac{2\Delta f^2}{f_0^3} \right] \quad \text{where}$$

Substituting $v_\ell = 3 \times 10^8$ m/sec, $\int N d\ell = 10^{19}$ el/m^2 and $f_0 = 2.45$ GHz, we find

$$\Delta\varphi_A - \Delta\varphi_B = 2\pi \times (1.8 \times 10^{-16}) \times \Delta f^2$$

for $\Delta\varphi_A - \Delta\varphi_B \leq 2\pi$

$$\Delta f^2 < \frac{1}{1.8 \times 10^{-16}} \quad \& \quad \Delta f^2 < 5.55 \times 10^{15}$$

$$\Delta f < 74 \text{ MHz.}$$

Thus, the approach described in the next section would resolve the 2π ionospheric ambiguity for frequency separations upwards of 70 MHz.

3.3.3 POSSIBLE APPROACHES FOR THE CORRECTION OF IONOSPHERIC INDUCED AMBIGUITIES IN THE SPS PILOT BEAM SYSTEM

3.3.3.1 Introduction

The removal of the ionospheric bias from the SPS pilot beam measurements (that are necessary for the accurate pointing of the downcoming SPS power beam) is a relevant undertaking from the standpoint of the overall performance of the pilot beam system.

In fact, if this bias is removed, the phase fluctuations induced by ionospheric turbulence in the pilot beam links can be dealt with effectively by performing time averages.

We present several possible approaches for the removal of the ionospheric bias and the alleviation, in general, of the ionospheric induced errors. Approach No. 1 is a rearrangement of the Doppler cancelling scheme that was successfully tested in space on the occasion of the gravitational red-shift rocket probe experiment conducted from Wallops Island on June 18, 1976 (Vessot and Levine, 1976). This approach uses two upgoing and one downcoming coherent frequencies. Approach No. 2 is a variation of the three-frequency scheme (Eshleman et al, 1960; Burns and Fremouw, 1970). Approach No. 3 is a Raytheon scheme that uses three upgoing frequencies and measures differential group delays (differently from what all of the above schemes do) in addition to performing phase measurements.

As already mentioned, Approach No. 1 and Approach No. 2 use solely phase measurements. They would therefore suffer from the difficulties pointed out in Section 3.3.2 of this report should the frequencies used in the related systems be too widely separated. In Approach No. 1 and Approach No. 2, these frequencies must be kept, in fact, within 1 MHz from each other in order to avoid the 2π ambiguity.

Approach No. 3, by adding differential group delay measurements, totally eliminates the problem created by the 2π ambiguity, thus removing the requirement of using closely spaced frequencies.

3.3.3.2 Approach No. 1

The basic principle of operation of this approach is given in Figure 3.5. Essentially, at the center of the SPS array (Reference Point) there is an inverted transponder that is linked, two-way, with a transponder at the ground station. The spaceborne inverted transponder is complemented with an additional receiver of a third link (upgoing).

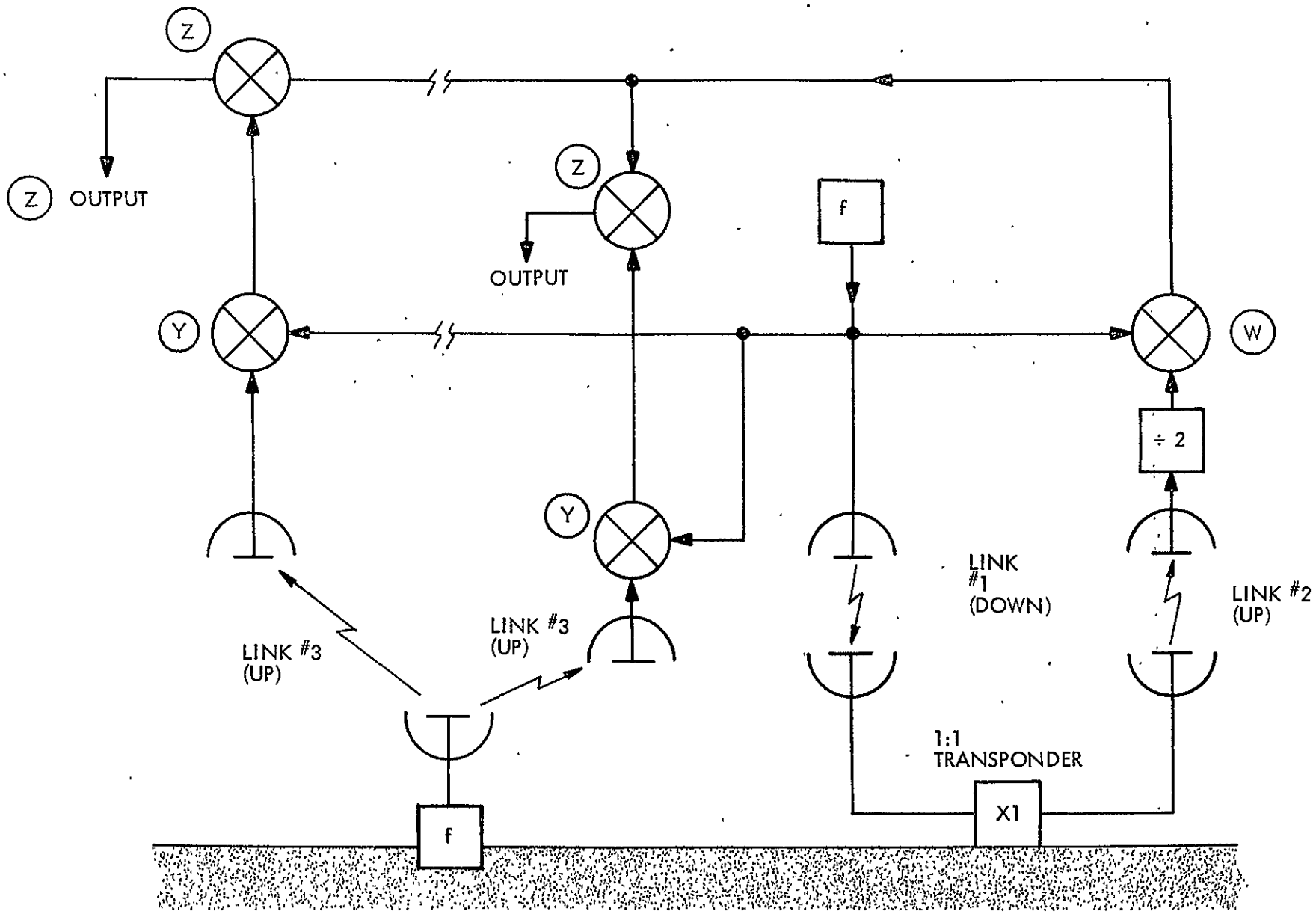

Figure 3.5. Simplified Block Diagram of Approach No. 1

At the nth measuring point of the array, we could have only a receiver (for the up-going Link # 3). More conservatively, we could have the complete three-frequency system at most points and the Link # 3 receiver at all points (or a dual-frequency receiver, for Link # 3 and Link # 1) or ultimately, the complete three-frequency system at all points. Adoption of the more complex alternatives would make it possible to cancel the effects of ionospheric horizontal gradients (wedges, sporadic E slabs, etc.) that might involve the path to the reference point but not the path to the nth measuring point. To see how the principle works, let's consider first the situation at the reference point : Let's call Φ_{OSPS} the phase at epoch 0 of the spaceborne master oscillator of the pilot beam system and Φ_{OG} the phase, at the same epoch, of the ground-based master oscillator used in Link # 3.

The phase of Link #1, on arrival at the ground site, is

$$\Phi_{0SPS} + \frac{2\pi}{v_\ell} [f L - \frac{40}{f} \int N dl]$$

where

v_ℓ is the velocity of light in free space

f is the frequency of the oscillator

L is the geometric distance from ground site to reference point

$\int N dl$ (el/m^2) is the columnar electron content from ground site to reference point.

Because the phase path length for Link #2 is

$$\frac{2\pi}{v_\ell} [fL - \frac{40}{f} \int N dl]$$

we have that the phase on arrival back to the SPS (after a two-way trip) is

$$\Phi_{0SPS} + \frac{2\pi}{v_\ell} [2 f L - 2 \cdot \frac{40}{f} \int N dl]$$

and after dividing by two:

$$\frac{\Phi_{0SPS}}{2} + \frac{2\pi}{v_\ell}\left[f\,L - \frac{40}{f}\int N\,dl\right]$$

At mixer W we subtract the phase at the new epoch 1 of the master oscillator output and we obtain therefore:

$$\frac{\Phi_{0SPS}}{2} - \Phi_{1SPS} + \frac{2\pi}{v_\ell}\left[f\,L - \frac{40}{f}\int N\,dl\right]$$

This waveform goes to the mixer Z. To the same mixer arrives (for subtraction) the phase arriving via Link #3

$$\Phi_{0G} + \frac{2\pi}{v_\ell}\left[f\,L' - \frac{40}{f}\int N\,dl\right]$$

from which at the mixer Y we have subtracted Φ_{1SPS}.

Therefore, at the output of Z we have

$$\Phi_{0G} + \frac{2\pi}{v_\ell}\left[f\,L - \frac{40}{f}\int N\,dl\right] - \Phi_{1SPS} - \left\{\frac{\Phi_{0SPS}}{2} - \Phi_{1SPS} + \frac{2\pi}{v_\ell}\left[f\,L - \frac{40}{f}\int N\,dl\right]\right\} = \Phi_{0G} - \frac{1}{2}\,\Phi_{0SPS}$$

We will use later on this quantity that we have obtained on the reference point.

It can be easily shown that the Z output for the nth measuring point, away from the center of the array and displaced of the quantity ΔL_n from the correct alignment, is:

$$\Phi_{0G} - \frac{1}{2}\,\Phi_{0SPS} + \frac{2\pi}{v_\ell}\left[f(L + \Delta L_n) - \frac{40}{f}\int N\,dl\right] - \Phi_{1SPS} + \Phi_{1SPS} - \frac{2\pi}{v_\ell}\left[f\,L - \frac{40}{f}\int N\,dl\right] = \left(\Phi_{0G} - \frac{1}{2}\,\Phi_{0SPS}\right) + \frac{2\pi}{v_\ell} f\,\Delta L_n$$

We can remove from this output the quantity in parenthesis, that was obtained at the reference point, and we have the term $\frac{2\pi}{v_\ell} f \Delta L_n$ that is all that we need to compute the wanted angular error of the vector{(reference point) -to-(n^{th} measuring point)}.

For practical reasons, we cannot implement the block diagram of Figure 3.5. We must in fact avoid front-to-back interferences in the ground transponder and in the spaceborne inverted transponder.

The block diagram in Figure 3.6 obviates these difficulties and is realizeable.

The new expression for the various phases are as follows (reference point case):

- Arriving phase on the ground, Link #1:

$$b\,\Phi_{0SPS} + \frac{2\pi}{v_\ell}\left[b\,f\,L - \frac{40}{bf}\int N\,dl\right]$$

- Departing phase from the ground, Link #2:

$$a\,b\,\Phi_{0SPS} + \frac{2\pi}{v_\ell}\left[a\,b\,f\,L - \frac{40}{f}\,\frac{a}{b}\int N\,dl\right]$$

- Arriving phase in space, Link #2:

$$a\,b\,\Phi_{0SPS} + \frac{2\pi}{v_\ell}\left[2\,a\,b\,f\,L - \frac{40}{bf}\,(a + 1/a)\int N\,dl\right]$$

- Phase entering mixer W from Link #2:

$$\frac{ab}{2}\,\Phi_{0SPS} + \frac{2\pi}{v_\ell}\left[abfL - \frac{40}{2bf}\,(a + 1/a)\int N\,dl\right]$$

- Output of mixer W:

$$\frac{ab}{2}\,\Phi_{0SPS} - ab\,\Phi_{1SPS} + \frac{2\pi}{v_\ell}\left[abfL - \frac{40}{2bf}\,(a + 1/a)\int N\,dl\right]$$

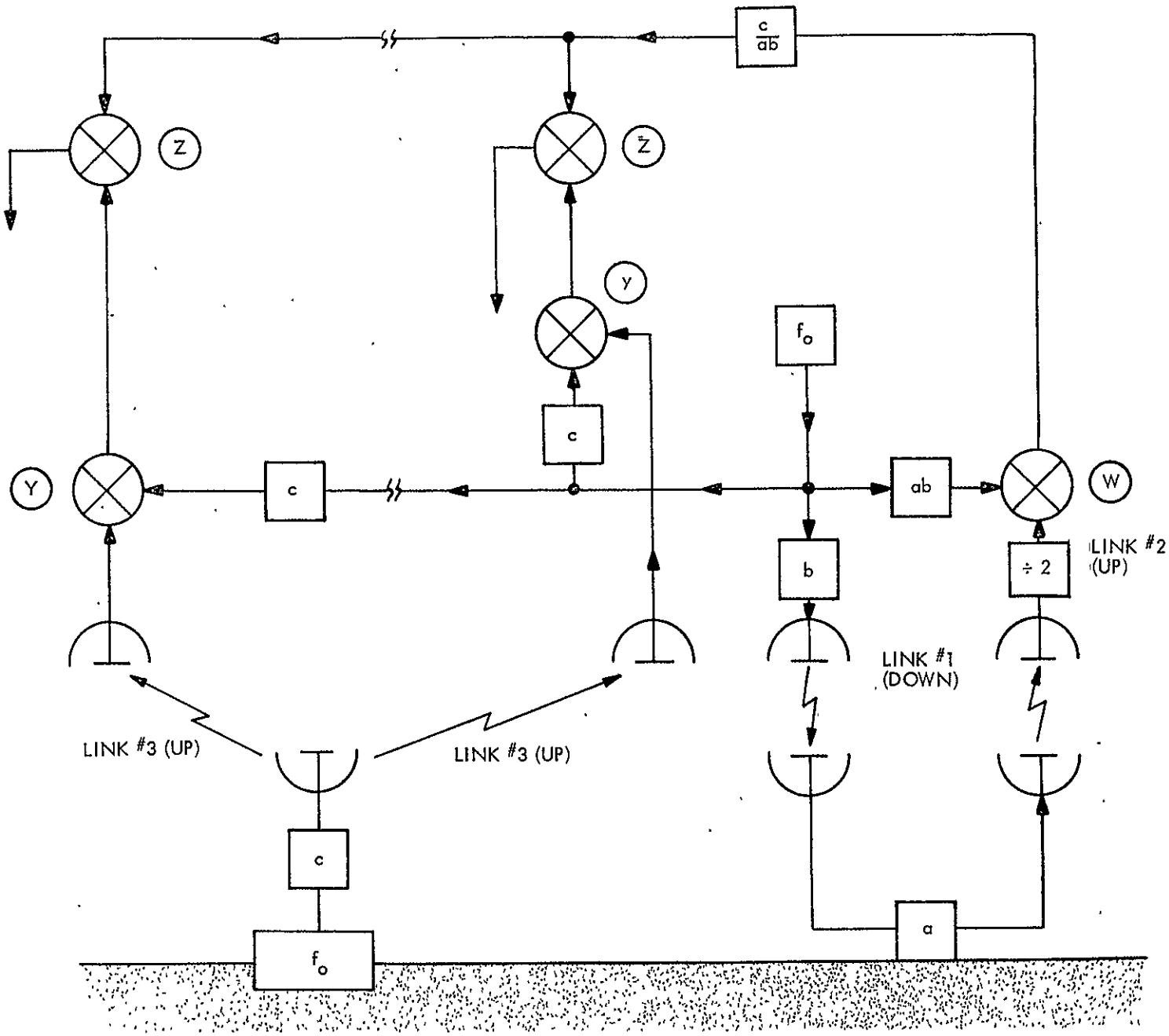

Figure 3.6. Block Diagram of Realizable System for Approach No. 1

- Phase entering mixer Z after multiplication by c/ab:

$$\frac{c}{2}\,\Phi_{0SPS} - c\,\Phi_{1SPS} + \frac{2\pi}{v_\ell}\left[cfL - \frac{40c}{2ab^2 f}(a + 1/a)\int N\,dl\right]$$

- Phase entering from Link #3 mixer Z (for subtraction) after going through addition of Φ_{1SPS} at mixer Y:

$$c\,\Phi_{0G} - c\,\Phi_{1SPS} + \frac{2\pi}{v_\ell}\left[cfL - \frac{40}{cf}\int N\,dl\right]$$

- Output of mixer Z:

$$c\,\Phi_{0G} - c\,\Phi_{1SPS} + \frac{2\pi}{v_\ell}\left[cfL - \frac{40}{cf}\int N\,dl\right] + c\,\Phi_{1SPS} - \frac{c}{2}\,\Phi_{0SPS}$$

$$- \frac{2\pi}{v_\ell}\left[cfL - \frac{40c}{2ab^2 f}(a + 1/a)\int N\,dl\right] = \left(c\,\Phi_{0G} - \frac{c}{2}\,\Phi_{0SPS}\right)$$

$$+ \frac{2\pi}{v_\ell}\left\{-\frac{40}{f}\int N\,dl\left[\frac{1}{c} - \frac{1}{2}\frac{c}{b^2}(1 + 1/a^2)\right]\right\}$$

- By making

$$\frac{1}{c} - \frac{1}{2}\frac{c}{b^2}(1 + 1/a^2) = 0$$

we have that the output of mixer Z is

$$c\left[\Phi_{0G} - \frac{1}{2}\,\Phi_{0SPS}\right]$$

This, apart from the constant c, is what we had got with the block diagram of Figure 3.5.

At the nth measuring point in the array we have:

- Phase entering mixer Z after multiplication by c/ab remains the same expression as for the reference point:

$$\frac{c}{2}\,\Phi_{0SPS} - c\,\Phi_{1SPS} + \frac{2\pi}{v_\ell}\left[cfL - \frac{40c}{2ab^2f}\left(a + \frac{1}{a}\right)\int N\,dl\right]$$

- Phase entering same mixer Z from Link #3 after subtraction of $c\,\Phi_{1SPS}$ at mixer Y is:

$$c\,\Phi_{0G} - c\,\Phi_{1SPS} + \frac{2\pi}{v_\ell}\left[cf(L + \Delta L_n) - \frac{40}{cf}\int N\,dl\right]$$

- At the output of mixer Z we have:

$$c\,\Phi_{0G} - c\,\Phi_{1SPS} + \frac{2\pi}{v_\ell}\left[cf(L + \Delta L_n) - \frac{40}{cf}\,N\,dl\right] - \frac{c}{2}\,\Phi_{0SPS}$$

$$+ c\,\Phi_{1SPS} - \frac{2\pi}{v_\ell}\left[cfL - \frac{40c}{2ab^2f}\left(a + \frac{1}{a}\right)\int N\,dl\right.$$

$$= c\left(\Phi_{0G} - \frac{1}{2}\,\Phi_{0SPS}\right) + \frac{2\pi}{v_\ell}\left(c\,f\,\Delta L_n\right)$$

if, as before, we make

$$\frac{1}{c} - \frac{1}{2}\,\frac{c}{a^2}\left(1 + \frac{1}{a^2}\right) = 0$$

- By removing from this Z output the term in parenthesis

$$c\left(\Phi_{0G} - \frac{1}{2}\,\Phi_{0SPS}\right)$$

we remain with the wanted quantity

$$\frac{2\pi}{v_\ell}\left(c\,f\,\Delta L_n\right)$$

From this quantity we can directly obtain the angular error of the vector {(reference point)-to-(n^{th} measuring point)}with respect to the wanted alignment. This quantity is to be used as input to the phase correction process.

To conclude, we submit that with the proposed approach we can accomplish the following:

A) Alternative #1

Transponder loop only at reference point, Link #3 receiver at reference point at all measuring points:

- We eliminate ionospheric bias.
- We eliminate horizontal gradients (wedges, etc.) that have a scale size large enough to involve all three link paths simultaneously.
- We make it possible to apply averaging processes (with a few seconds integration time) and thus strongly reduce the effect of random turbulence in the ionosphere.

B) Alternative #2

Complete system (transponder loop and Link #3 receiver) at most points. Link #3 receiver at all points.

- We eliminate ionospheric bias as before.
- We make it possible, as before, to apply averaging processes (with a few seconds integration time) and thus strongly reduce the effect of random turbulence in the ionosphere.
- Different from before, we eliminate all effects of small size horizontal gradients (wedges, etc.).

3.3.3.3 APPROACH #2

Reference is made to Figure 3.7. By calling Φ_o the common phase of origin at the ground site (Φ_o could be easily made equal to zero without any loss of generality), the expressions of the phases arriving at the reference point are:

$$\Phi_1' = a\,\Phi_0 + \frac{2\pi}{v_\ell}\left(afL - \frac{40}{af}\int N\,dl\right)$$

$$\Phi_2' = b\,\Phi_0 + \frac{2\pi}{v_\ell}\left(bfL - \frac{40}{bf}\int N\,dl\right)$$

$$\Phi_3' = c\,\Phi_0 + \frac{2\pi}{v_\ell}\left(cfL - \frac{40}{cf}\int N\,dl\right)$$

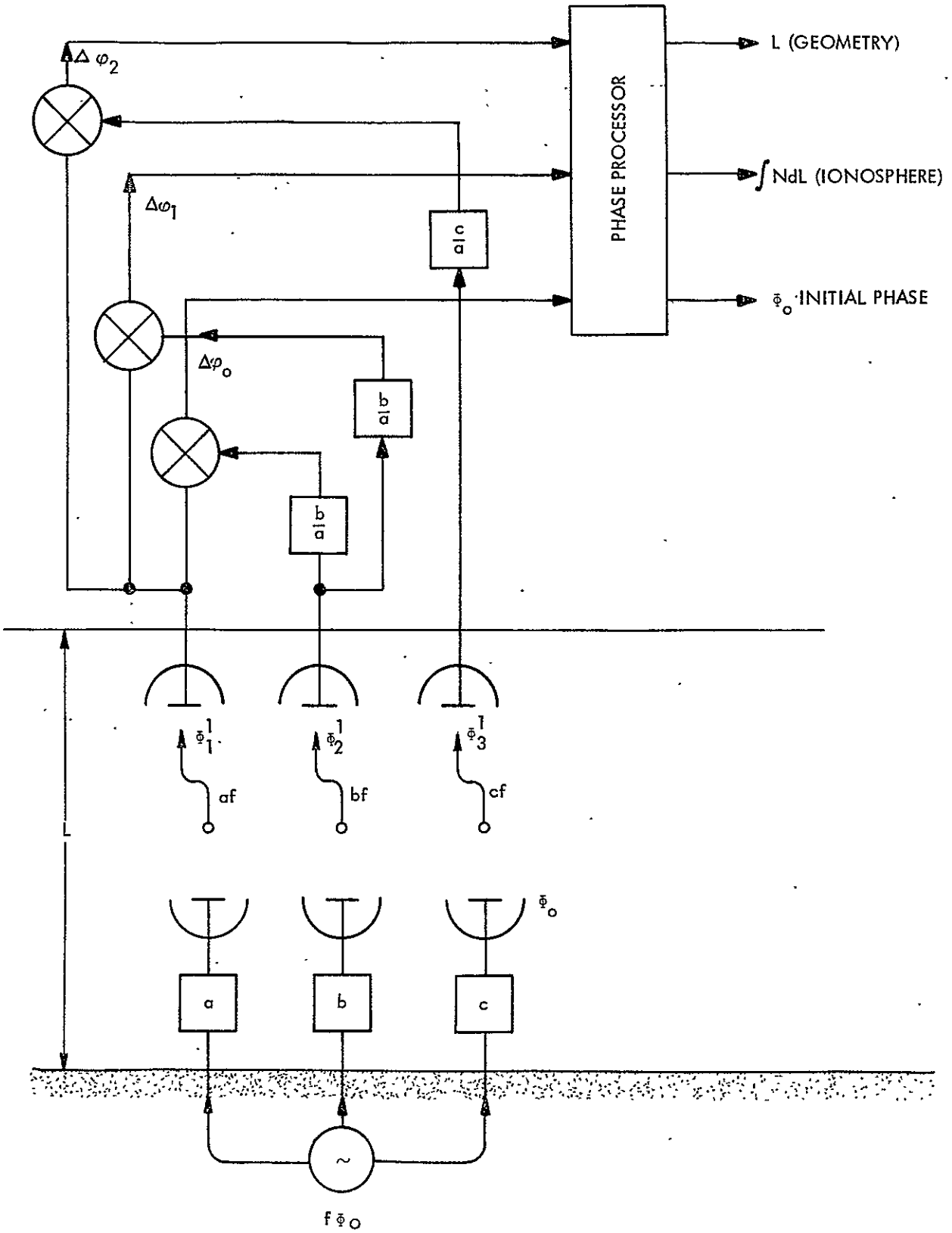

Figure 3.7. Block Diagram of Approach No. 2

We perform on them the following mathematical operations:

$$\Delta \phi_0 = \Phi_1' - \frac{a}{b} \Phi_2' = \frac{2\pi}{v_\ell} \left(\frac{a}{b^2} - \frac{1}{a} \right) \frac{40}{f} \int N \, dl$$

$$\Delta \phi_1 = \Phi_1' - \frac{b}{a} \Phi_2' = \left(a - \frac{b^2}{a} \right) \Phi_0 + \frac{2\pi}{v_\ell} \left(a - \frac{b^2}{a} \right) fL$$

$$\Delta \phi_2 = \Phi_1' - \frac{c}{a} \Phi_3' = \left(a - \frac{c^2}{a} \right) \Phi_0 + \frac{2\pi}{v_\ell} \left(a - \frac{c^2}{a} \right) fL$$

and we rewrite them as follows:

$$\Delta \phi_0 = K_0 \int N \, dl$$

$$\Delta \phi_1 = K_1 \Phi_0 + K_2 L$$

$$\Delta \phi_2 = K_3 \Phi_0 + K_4 L$$

By solving this system of equations, we obtain:

$$L = \frac{K_3 \Delta \phi_1 - K_1 \Delta \phi_2}{K_2 K_3 - K_1 K_4}$$

$$\Phi_0 = \frac{K_4 \Delta \phi_1 - K_2 \Delta \phi_2}{K_1 K_4 - K_2 K_3}$$

$$\int N \, dl = \frac{1}{K_0} \Delta \phi_0$$

This process can be repeated at any other point on the array.

Therefore, at any measuring point we have all the quantities that are necessary for the determination of the SPS phase correction coefficients. By distributing the L parameter from the reference point to all measuring points, it is possible to determine the quantity ΔL for each one of the measuring points, thus determining the geometric misalignment of the SPS array from the wanted position.

Approach #2 is simpler because it does not require pilot beam transmitters onboard the SPS. In addition, it is not sensitive to temporal changes of the ionospheric conditions during the round trip time, ground-SPS-ground, that on the contrary still affects Approach #1.

The method corrects for the ionospheric columnar content $\int N\,dl$, for horizontal gradients of scale size arbitrarily small and makes it possible to deal with the phase scintillations due to ionospheric turbulence by averaging them out (averaging time of a few seconds). As indicated in Section 1, the method is, however, sensitive to the 2π ambiguity. This must be obviated by choosing triplet of frequencies very close together (within approximately 1 MHz).

3.3.3.4 APPROACH #3

This approach consists of the use of 3 (or 4) upgoing frequencies, 1 (or 2) CW, two pulse-modulated, and in the performance of differential group delay measurements with the pulsed links and of phase measurements with the CW ones.

The principle of operation is as follows.

If we transmit from the ground site of the pilot beam system two frequencies, f_1 and f_2, pulse-modulated, we can measure onboard SPS the differential time delay (difference in time of arrival of the two pulses). The following formula applies

$$\Delta\tau = \underset{\text{(in seconds)}}{\text{Differential Group Delay}} = \frac{40}{c}\left(\frac{1}{f_1^2} - \frac{1}{f_2^2}\right)\int N\,ds$$

where c is the velocity of light in free space (m/sec), N is the ionospheric electron density in el/m^3, f is the frequency in Hz.

From the above equation, we can derive $\int N\,ds$ without any ambiguity (2π or otherwise) and we obtain:

$$\int N\,ds = \frac{\Delta\tau\; f_1^2 f_2^2\; c}{40\left(f_2^2 - f_1^2\right)}$$

(The two pulses leave ground exactly at the same time)

This numerical quantity is computed by the onboard processor and is updated each time that a pair of pulses arrives (for instance, once a second). The measurements are performed at the reference point and at all, or most, of the measurement points.

By subtracting this quantity from the phase that arrives at each point, we remain only with the effect of geometrical length. At the initial calibration (and periodic checks) of the SPS orientation, the front of the arriving wave would be parallel to the alignment (apart from the distorsion of the structure, which is also measurable with our method) and the on-board processor would track any phase rotation from now on without 2π ambiguity.

This method has therefore all the attractive characteristics of Approach #2 with the added feature of the lack of ambiguities and without imposing the need for closely allocated frequencies.

3.3.3.5 CONCLUSIONS

We can conclude from the above that the ionosphere (apart from possible effects of the heating due to the SPS power beam) should not be considered as a potential program stopper.

Substantial work, of course, is still necessary in order to complete the conceptual development of the several schemes illustrated in the previous sections. However, it seems fully justified to state that at least one of the methods above will be found free from stumbling blocks.

This recommended additional work will also provide the basis for the design of ground-based experiments on the SPS pilot beam system, including an investigation of ionospheric effects (both natural and power-beam induced) on it.

3.4 PHASE ERRORS DUE TO IONOSPHERIC FLUCTUATIONS

3.4.1 STATEMENT OF THE PROBLEM

A key factor in the retrodirective phase control system is the assumption that the system automatically compensates for the phase-fluctuations attributed to the ionosphere. This assumption depends on there being path symmetry between the upgoing pilot beam and the downcoming power beam. Path symmetry requires both spatial and temporal symmetry.

Figure 3.8 illustrates the geometry of the downcoming power beam and the upgoing pilot beam. The pilot beam has an effective ionospheric interaction width which is much smaller than the ionospheric interaction width of the power beam. For straight line, ray geometry, the ionospheric interaction width of the pilot beam is determined by the angle 1 Km transmit array in GEO subtends the pilot beam from the ground. That is the -

Pilot beam interaction width = angular extend of the 1 Km array x height of ionospheric interaction region

$$= \frac{1 \text{ Km}}{37,500 \text{ Km}} \times \text{ionospheric height}$$

$$= 2.67 \times 10^{-5} \text{ radian} \times \text{ionospheric height.}$$

If the ionospheric height is 100 Km (1000 Km), the pilot beam ionospheric interaction width is 2.7 m (27 m).

This point is illustrated in the next two figures. Figure 3.9 shows an expanded view of the ionospheric interaction region with the width of the power beam and the 3 dB width of the pilot beam shown to scale (assuming a 30 aperture for the pilot beam). The line of sight width of the ionospheric interaction region varies from 3 to 30 m and is obviously not shown to scale.

The ionospheric induced phase front variations arise from two basic interactions. For small perturbations (3 to 10 meter irregularities) line-of-sight phase fluctuations occur and for the large scale perturbations amplitude fading and phase occur due to the interference pattern x of the direct and the scattered ray. In the latter case, the size of the irregularities that are significant is determined

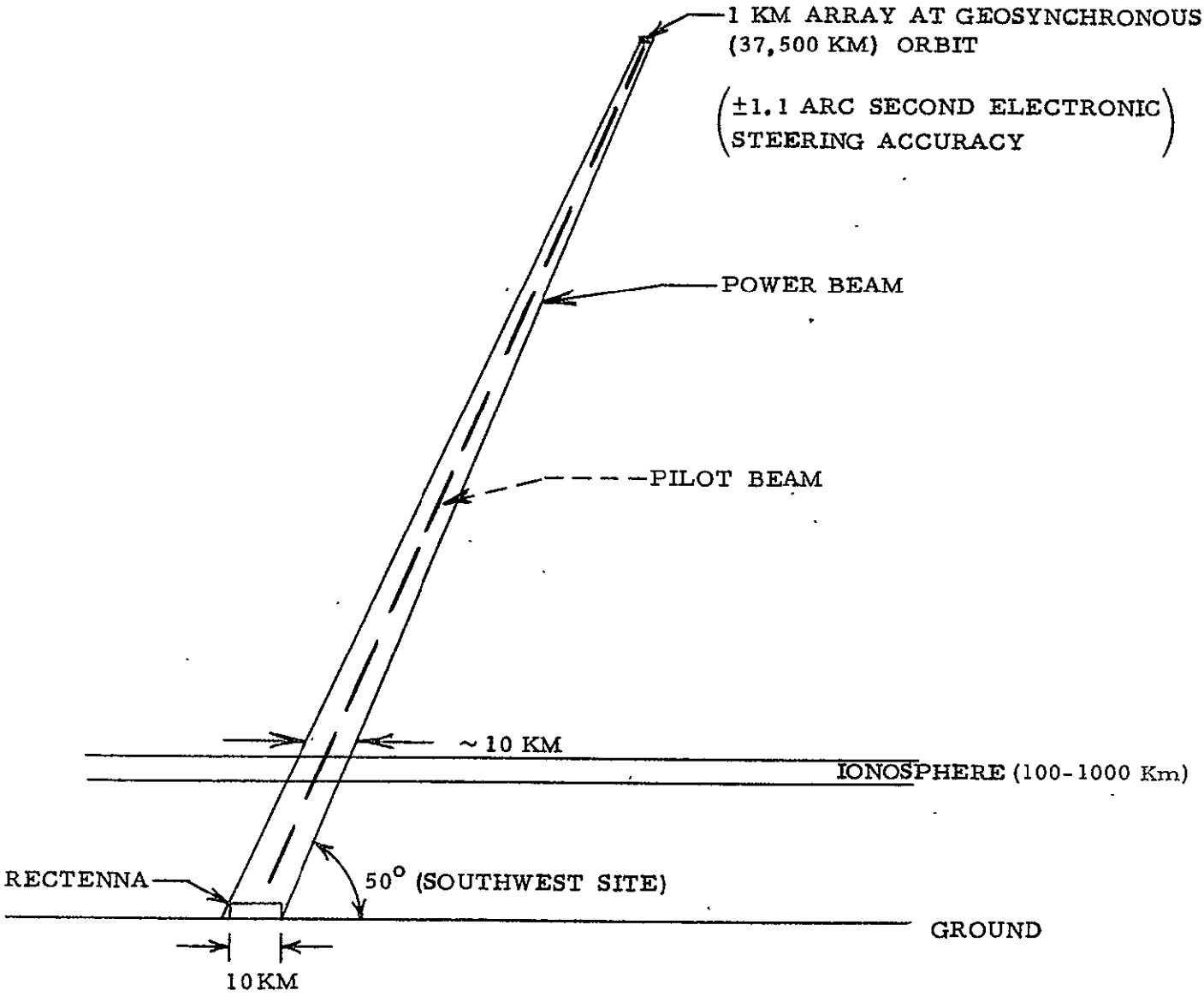

Figure 3.8. Schematic Representation of Power Beam and Pilot Beam

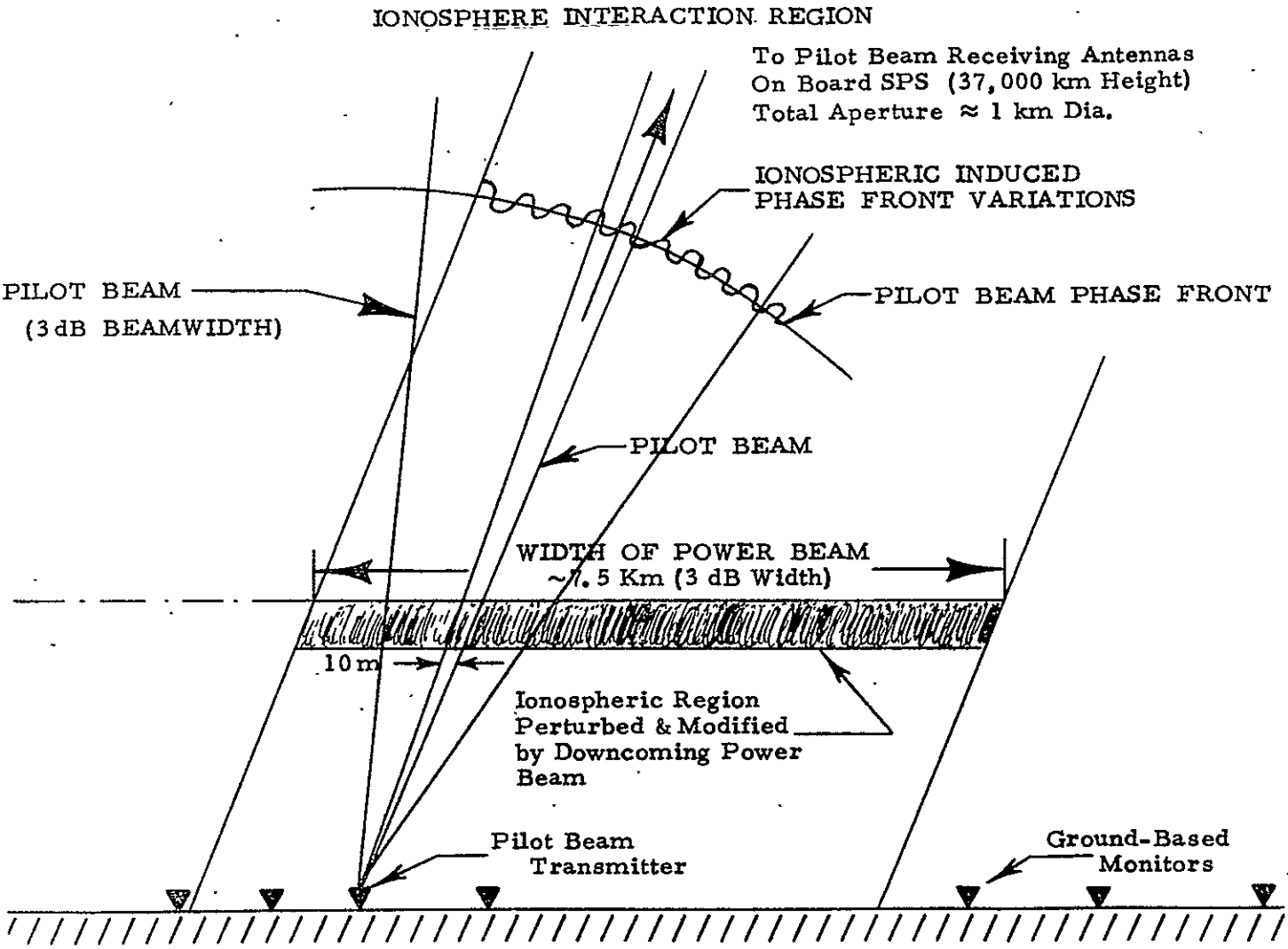

Figure 3.9. Expanded view of ionospheric interaction region for both pilot beam and power beam

by the Fresnel zone which for this geometry is between 200 and 400 m. Figure 3.9 shows that both interactions are likely to occur as the 3 dB width of the pilot beam signal is greater than the Fresnel zone.

The previous discussion illustrates that the upgoing pilot beam ionospheric interaction region is not equivalent with the downcoming power beam and as such, the retrodirective system which automatically conjugates the ionospheric phase perturbations of the upgoing pilot beam is not going to remove the ionospheric effects when the downcoming power beam passes through the ionosphere.

Figure 3.10 shows an expanded view of the pilot beam interaction region. Ionization irregularities with characteristic wavelengths between 3 to 10 m are shown moving horizontally through the interaction region with speeds up to 50 m/sec. Thus, the phase perturbation caused by these small scale irregularities will temporally fluctuate on the time scale of less than 0.1 second. As the round trip time delay from the ground to GEO is 0.25 seconds, we see that the phase fluctuations due to the ionosphere could not be automatically compensated for by the retrodirective phase control system because the time constant of the retrodirective phase control system is longer than the time constant of the ionosphere. The time constant for the retrodirective phase control system is the round trip time delay of 0.25 seconds.

The basic assumption of the baseline retrodirective phase control system, at least with respect to the ionosphere, requires path symmetry between the pilot beam and the power beam and ionospheric time stabilities longer than 0.25 sec. We have shown that neither of these assumptions is valid. The next step in the analysis is to determine if the magnitude of the ionospheric phase errors on the SPS power beam is large enough to exceed system specifications and, if so, to investigate alternate concepts or mitigating strategies for reducing the ionospheric effects.

3.4.2 EFFECTS OF PHASE ERRORS ON THE SPS POWER BEAM

The effect of random phase errors across the transmit array at GEO is to reduce beam efficiency, reduce beam pointing accuracy, and increase sidelobe levels. The rms phase error budget for the baseline is 13° exclusive of propagation. This section will describe the impact the addition of the ionospheric induced phase error fluctuations will have on SPS performance.

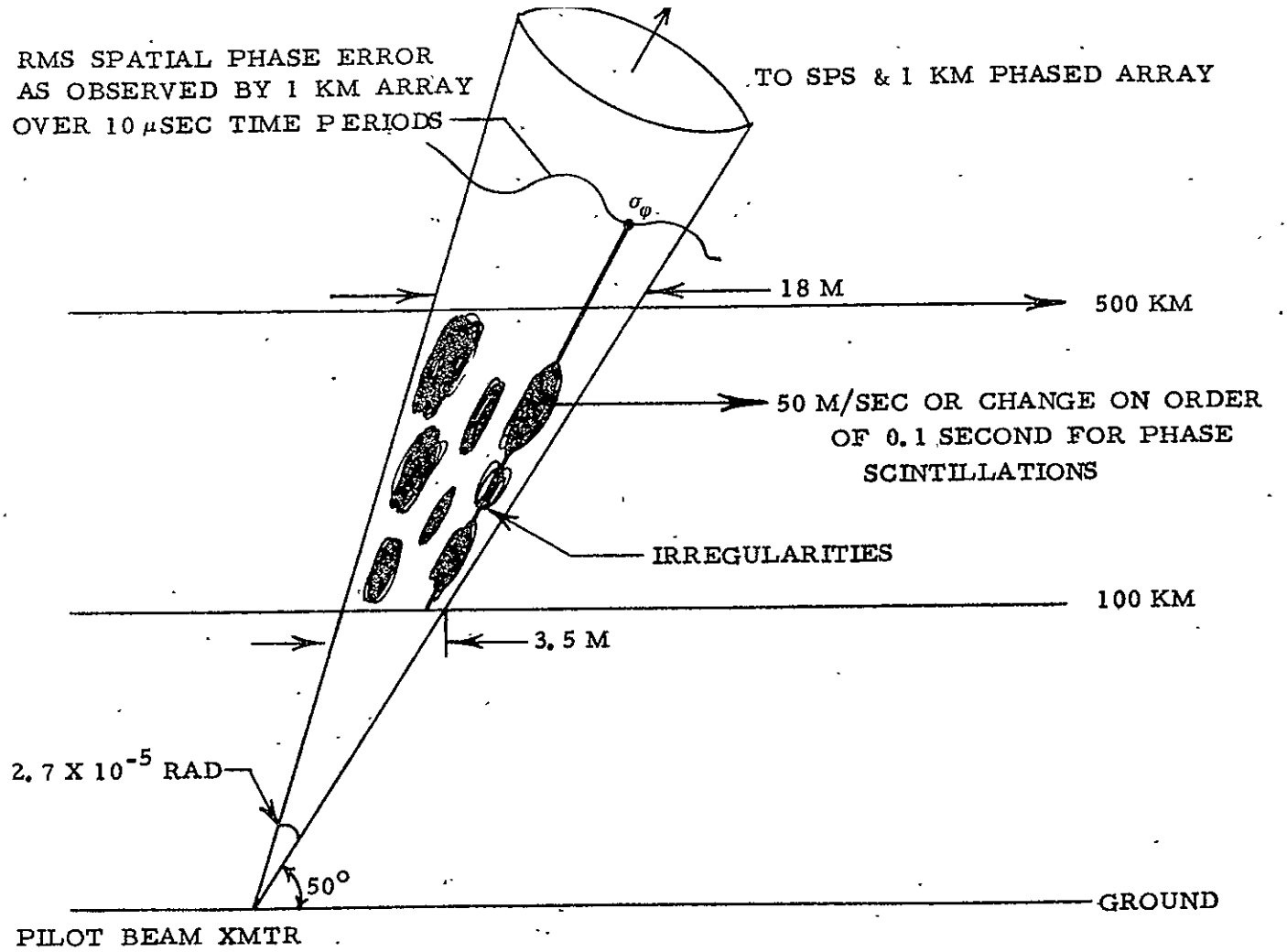

Figure 3.10. Expanded view of ionospheric interaction region for pilot beam

3.4.2.1 Beam Efficiency

Figure 3.11 shows a plot of the reduced efficiency versus rms phase errors per subarray. The current baseline (13 degrees) exclusive of propagation is shown to reduce beam efficiency by approximately 6%. Section 3.2.3 indicated that rms phase errors up to 40° might be expected for ionospheric fluctuations. This does not indicate how often such ionospheric induced fluctuations will occur and further does not indicate the impact of the SPS power beam on the generation of these irregularities. Thus, although we can assess the magnitude of the ionospheric effects, we cannot yet fully assess their impact. If a large fluctuation occurs infrequently, then its impact might be relatively unimportant. A 40° contribution from the ionosphere reduces efficiently by approximately 33% which is 27% below the baseline.

The ionospheric induced phase errors, depending on their magnitude, have a significant impact on system performance vis-a-vis beam efficiency. However, it is not clear at the present time how often the large phase fluctuations occur and further, it is uncertain as to whether the SPS power beam ionospheric heating will significantly increase the occurrence and magnitude of the ionospheric induced phase errors.

The phase errors result in a reduced efficiency which results in a loss of power which will directly effect the cost of the power. A 24% loss of 5 GH of power is 1200 MW. An additional factor is that these losses will be varying with time on the order of 0.1 to 1 second. This could present a problem when delivering the energy to the power grid which expects a very constant source of power. Fluctuations of 10% in power delivered to the electrical power grid are probably unacceptable and will require engineering solutions to reduce these fluctuations. The engineering solutions could be composed of modifications to the pilot beam system (see Section 3.4.3) or modifications to the microwave to DC conversion which occurs at the rectenna. These issues will have to be explored in the Phase II study.

The results indicate the need to perform experiments during the GBER (Ground Based Experimental Research) Program which will measure the magnitude and the statistics of the ionospheric phase fluctuations.

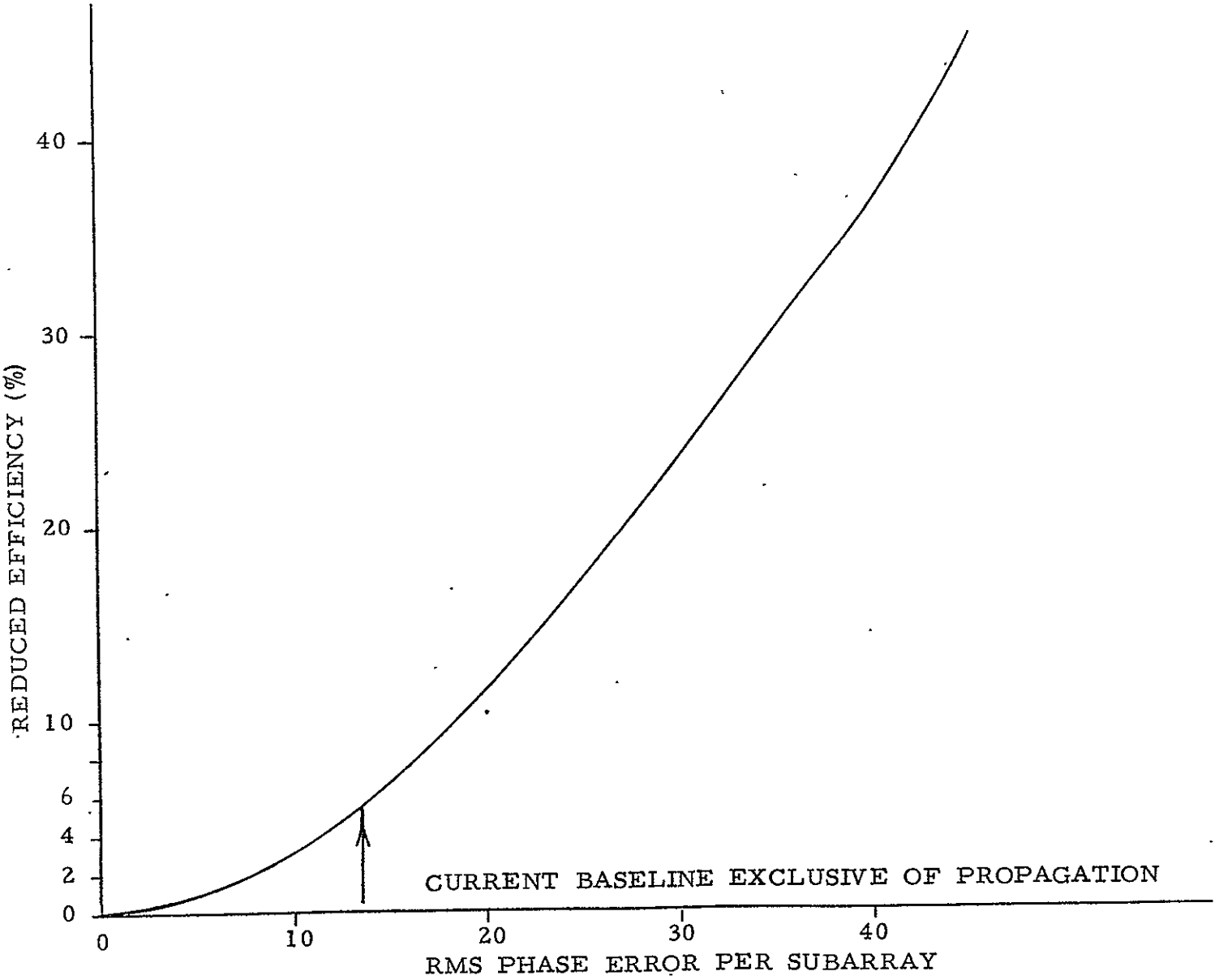

Figure 3.11. Reduction in Beam Efficiency ϕ vs rms Phase Error

3.4.2.2 Beam Pointing Accuracy

The one sigma rms pointing angle is determined by:

$$\sigma_\theta = \frac{0.5 \ \theta_{3\,dB} \ \sigma_\varphi}{\sqrt{N}}$$

$$\begin{cases} \sigma_\theta = \text{RMS POINTING ANGLE} \\ N = \text{NO. OF SUBARRAYS} \cong 1670 \\ \theta_{3\,dB} \sim \frac{\lambda}{D} \sim 1.5 \times 10^{-4} \text{ RAD} \\ \sigma_\varphi = \text{RMS PHASE ERROR PER SUBARRAY} \end{cases}$$

Figure 3.12 shows the effects of rms phase error on pointing angle. The baseline specification of 1 arc second is shown. The total 1 sigma phase error allowed is 166° which results in the requirement that the ionospheric induced phase fluctuations be less than 165°. As this is a factor of 4 greater than the maximum phase observed in the presently available data base, it is unlikely that ionospheric phase fluctuations will increase the pointing of the main beam above the baseline specification.

Of course, this will have to be verified during the GBER particularly in the presence of ionospheric perturbations arising from power beam heating effects. This also assumes that the ionospheric induced error is random across the array. This will also have to be verified during the GBER program.

3.4.2.3 Sidelobe Level

Figure 3.13 shows the beam pattern as a function of angle from boresight. The pattern is shown for a 10 m subarray with 13° rms phase errors. Including an ionospheric phase error contribution of 40° reduces the efficiency by an additional 24%. The close-in sidelobe levels (i.e., within its beamwidth a subarray) will increase by the power lost from the main beam times the ratio of the beamwidth of the subarray to the beamwidth of the main beam antenna. 24% loss in power efficiency results in a -6 dB power loss to the sidelobes and the ratio of the beamwidth of the 10 m subarray to the 1 Km array is approximately 10^{-4} (-40 dB). Thus, the sidelobes will be increased to 46 dB below the peak of the beam due to ionospheric phase errors of 40°. As can be seen from Figure 3.13, this will not have any effect on the sidelobes within 0.1 deg. from the boresight

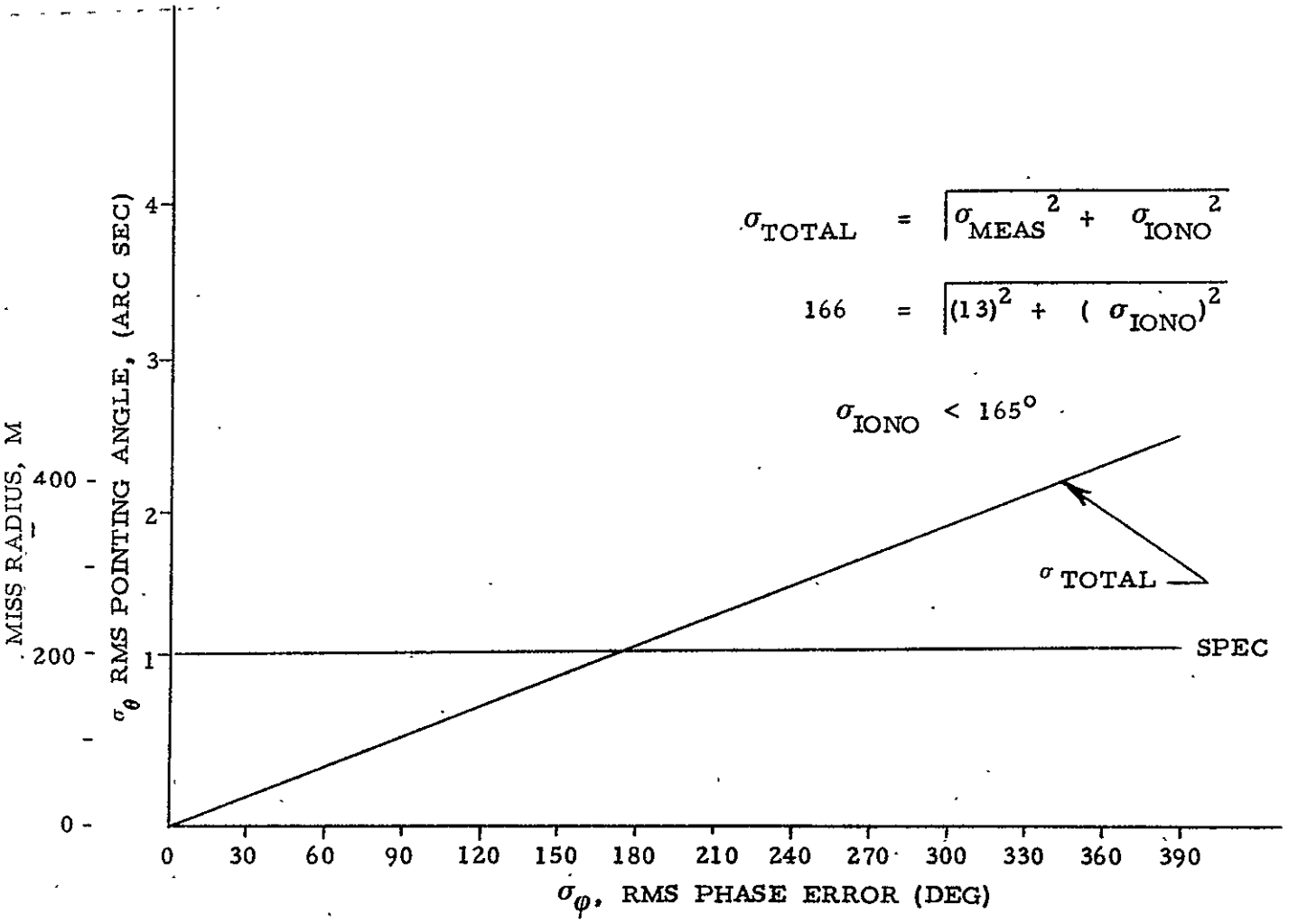

Figure 3.12. RMS Beam Pointing Angle vs RMS Phase Error

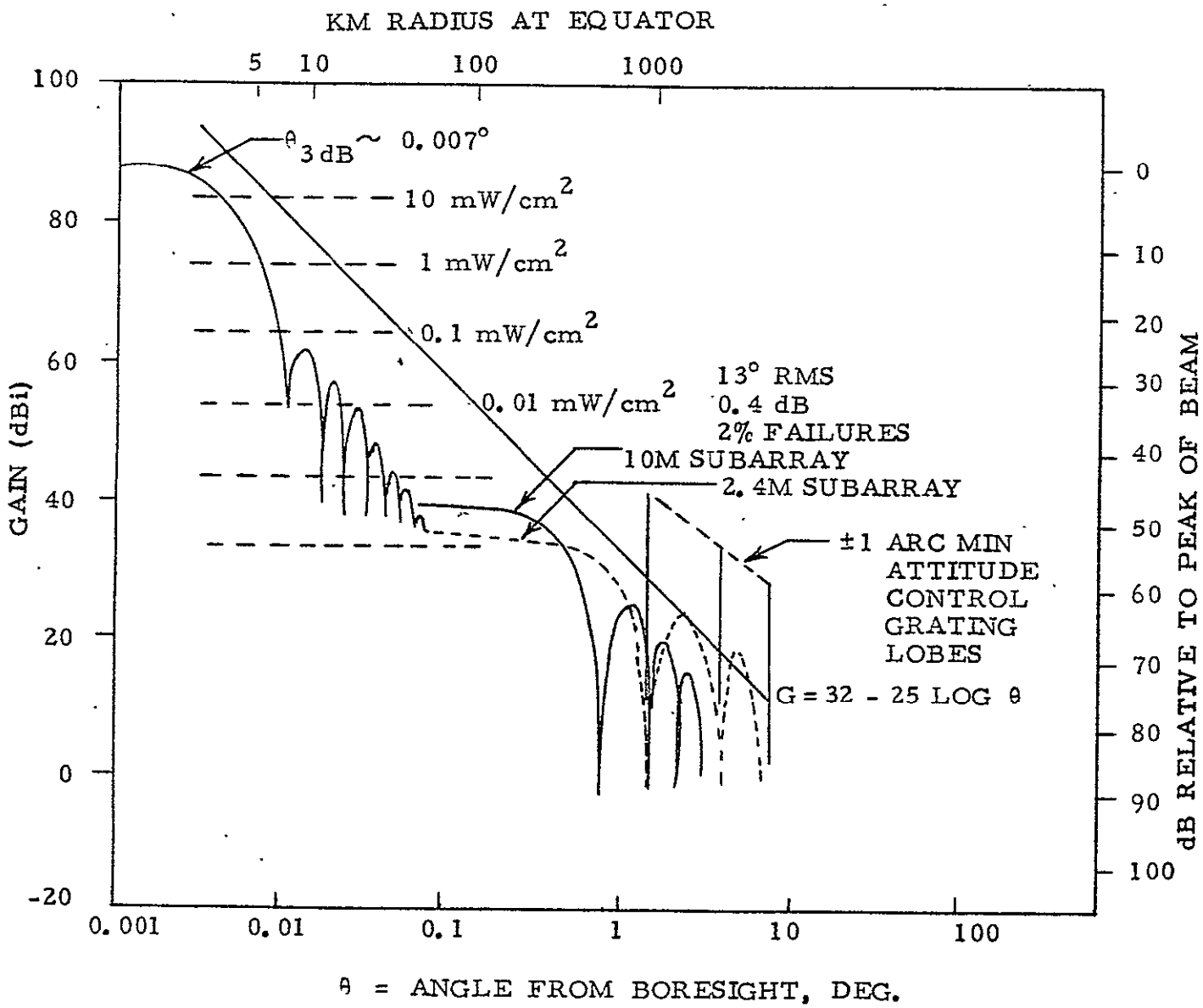

Figure 3.13. SPS Antenna Gain vs Angle From Boresight

and only increase the sidelobes by at most 3 dB between 0.1 and 1 degree off-boresight. At angles greater than 1 degree, the effect on the sidelobes will be even smaller because it is further reduced by the sidelobe levels of the 10 m subarray.

Thus, for the largest ionospheric phase error expected (excluding possible effects of power beam ionospheric heating), the increase in sidelobes due to ionospheric effects is not significant. This assumes that the ionospheric phase errors are randomly distributed across the 1 Km array. This factor will have to be verified during the GBER program.

3.4.3 MITIGATING STRATEGIES

It has been shown that the ionosphere poses a potential adverse impact on the SPS system. The classification of this as a potential program stopper depends both on the severity of the effects and on the likelihood of a mitigating strategy. The alternate pilot beam system described in Section 3.2.3 has substantially reduced the probability of the ionosphere, vis-a-vis the pilot beam system, being a program stopper. However, the rms ionospheric phase errors described in the previous sections could cause reductions in beam efficiency which would impact on both the econometrics of the SPS and on the integrability of its output power into the power grid. There are several mitigating procedures that could reduce the magnitude of the ionospheric induced phase fluctuations and thus increase beam efficiency and reduce the time variability of the output power. Table 3.2 lists several mitigating strategies that were investigated.

3.4.3.1 Spatial Diversity

The first strategy utilized two or more pilot beam transmitters for each SPS. The transmitters must be spaced so that the ionospheric region that each pilot beam intersects does not overlap or that the ionospheric induced phase fluctuations on each pilot beam are uncorrelated. Under this assumption, the rms phase fluctuations are reduced by (No. of XMTRs)$^{-1/2}$ if the average phase from each pilot beam is incoherently combined. However, to reduce a 40° phase error to 10° (a factor of 4) requires 16 individual pilot beam transmitters, which is unacceptable. Further, it would be difficult to adjust for the bias each pilot beam would have with respect to the central pilot beam system.

TABLE 3.2. MITIGATING STRATEGIES TO REDUCE IONOSPHERIC INDUCED PHASE FLUCTUATION

METHOD	IMPLEMENTATION	IMPROVEMENT
SPATIAL DIVERSITY	TWO OR MORE XMTRS ON GROUND SO PILOT BEAM TRAVERSES DIFFERENT IONOSPHERES	$\left(\text{NO. OF TRANSMITTERS}\right)^{-1/2}$
TEMPORAL DIVERSITY	AVERAGE PHASE FLUCTUATIONS IN TIME PERIOD LONG COMPARED TO STABILITY OF PROPAGATION PATHS	$\left(\frac{\text{INTEGRATION TIME}}{\text{IONOSPHERE TIME CONSTANT}}\right)^{-1/2}$
FREQUENCY DIVERSITY		
INCOHERENT	NOT APPLICABLE	PHASE FLUCTUATIONS TRACK INCOHERENT AVERAGE DOES NOT SIGNIFICANTLY IMPROVE PERFORMANCE
COHERENT	TRACK PHASE FLUCTUATIONS ON TWO FREQUENCIES OR THREE FREQUENCIES	

3.4.3.2 Temporal Diversity

In this approach the phase measurements from a single pilot beam are incoherently averaged over a time period long compared to the ionospheric time constant but short compared to the motion of the SPS satellite. The approach is particularly effective when used in conjunction with the pilot beam systems described in Section 3.3.3 which removes the 2π ambiguity due to the ionosphere. If the ionospheric times constant is on the order of 0.1 sec, then an incoherent integration time of 1.6 seconds would reduce the rms error by a factor of four. This will reduce the maximum 40 degree ionospheric phase errors to 10 degrees which is less than the baseline specifications of 13 degrees exclusive of propagation.

This solution is very attractive but requires a measurements program to determine the ionospheric time constants with respect to the pilot beam system and thus to determine optimum integration time.

3.4.3.3 Frequency Diversity

This approach has two possibilities. The first is an incoherent average of the phase fluctuations at two frequencies. This is discarded because fluctuations at each frequency track and an incoherent average does not reduce the phase fluctuations. However, the second possibility, a difference of phase fluctuations does indeed reduce the phase fluctuations. This, of course, requires that the 2π ambiguity, as described in Section 3.3.3, is removed before the differences in phase between the two frequencies is determined.

The difference in phase between two frequencies is determined as (see Section 3.2.1):

$$\Delta\varphi = \varphi_2 - \varphi_1 = \frac{2\pi}{v_\ell} 40 \int_l N dl \times \left[\frac{f_2}{f_1^{\,2}} - \frac{1}{f_2} \right]$$

$$f_2 = f_0 + \Delta f$$

$$f_1 = f_0 - \Delta f$$

Further, the difference in $\Delta\varphi$ due to fluctuations in $\int Ndl$ is:

$$\delta(\Delta\varphi) = \frac{2\pi}{v_\ell} 40 \underbrace{\delta\left(\int Ndl\right)}_{\substack{\text{fluctuation} \\ \text{in } \int Ndl}} \times \frac{f_2}{f_1^2} - \frac{1}{f_2}$$

Now, since $f_2 = f_0 + \Delta f$ and $f_1 = f_0 - \Delta f$, we find that

$$\delta(\Delta\varphi) \cong \frac{2\pi}{v_\ell} 40\, \delta\left(\int Ndl\right) \times \frac{2\Delta f}{f_0^2}$$

$$\cong \underbrace{\frac{2\pi}{v_\ell} 40\, \delta\left(\int Ndl\right) \times \frac{1}{f_0}}_{\substack{\text{rms phase error due to} \\ \text{change in ionosphere at} \\ f_0}} \times \underbrace{\frac{2\Delta f}{f_0}}_{\substack{\text{reduction} \\ \text{in phase} \\ \text{error if two} \\ \text{frequencies} \\ \text{used}}}$$

Thus, if $\Delta f = 100$ MHz, then $\frac{2\Delta f}{f_0} \sim 0.1$ and we find rms fluctuations of $40°$ reduced to $4°$ which is smaller than the $13°$ baseline. This approach assumes that the 2π ambiguity has been resolved.

3.5 RECOMMENDATIONS FOR PHASE III

Several different approaches to the pilot beam system and mitigating strategies to reduce effects of ionosphere have been developed under the Phase I study.

1. An Engineering Ionospheric Model is required for Evaluation of these Pilot Beam Systems and Mitigating Strategy. The first task of the Phase II study is to complete the Engineering Ionospheric Model. This will include:

   a. Completing the modeling of the ionospheric wedge and adding it to the 3-dimensional smooth ionospheric model;

   b. Performing the modeling of the phase perturbations induced by natural ionospheric irregularities based on the Refractive Scattering approach;

   c. Constructing an initial model of the phase perturbations induced by artificial ionospheric irregularities caused by the SPS beam;

   d. Augmenting the contents of the Data Base by bringing in recent, yet unpublished, observational results;

   e. Constructing an updated overall spectral density curve (y-axis : fractional change in electron density, $\frac{\delta n}{n} / \sqrt{K_m^{-1}}$; x-axis : wave number) in the spatial wavelength interval from 3 m to 1 Km

   f. Constructing an initial example of probability distribution curve (y-axis : percentage of time for which an ionosphere induced phase error exceeds the value read in the X-axis).

2. Multi-Frequency pilot beam system approaches are in principle applicable to the removal of the ionospheric bias that goes uncorrected in the current (Oct. 1978) dual frequency baseline pilot beam system. To assess these approaches the following tasks are recommended:

a. Complete conceptual development of the alternate pilot beam approaches which remove the ionospheric bias from the SPS pilot beam system.

b. Test these schemes using the Engineering model developed in Task I.1. (containing the model of the 3-dimensional wedge).

c. Identify the SPS system modifications which will be necessary to incorporate the alternate approaches into the pilot beam system.

d. Identify the overall most promising approaches to the pilot beam system.

3. Phase errors due to ionospheric fluctuations have been shown to significantly reduce the overall efficiency up to approximately 24%) of the SPS power transmission. Mitigating strategies have been proposed which should significantly reduce the impact of the ionospheric induced phase fluctuations. To assess these mitigating strategies, the following tasks are recommended:

   a. Test the mitigating strategies developed to reduce ionospheric fluctuations by using the ionospheric model developed in Task I. 1.

   b. Identify system modifications required to incorporate recommended mitigating strategies into the SPS pilot beam system.

   c. Identify the most promising mitigating strategies.

4. The analysis performed above will depend on ionospheric models, although obtained from the best available information to date. Therefore, we will need to verify our conclusions, particularly with respect to the effects of the SPS power beam ionospheric heating and with respect to the statistical distribution or occurrence of the ionospheric fluctuations. Furthermore, the data base used was not collected for direct application to the SPS pilot beam system. For this reason, the last task of the pilot beam-ionospheric study will be to establish the requirements as well as experimental test configurations to be implemented during the GBER; ionospheric models as related to pilot beam system; recommended phase control approaches; and mitigating strategies to reduce ionospheric-induced phase fluctuations.

3.6 REFERENCES

Crain, C. and Booker, H. G., "Use of Refractive Scattering to Explain SHF Scintillations," to be submitted for publication 1978.

Basu, S. and Kelley, M. C., "Review of Equatorial Scintillation Phenomena in Light of Recent Developments in the Theory and Measurement of Equatorial Irregularities," J. Atmos. and Terres. Physics, Vol. 39, No. 9/12, p 1229-1242, 1977.

Costa, E. and Kelley, M. C., "Calculations of Equatorial Scintillation at UHF and GHz Frequencies Based on a New Model of the Disturbed Equatorial Ionosphere," Geophys. Res. Lett. 3, 677-680, 1976.

Costa, E. and Kelley, M. C., "Ionospheric Scintillation Calculations Based on In-Situ Irregularity Spectra," Radio Science 12, p 797-811, 1977.

Basu, Sunanda et al, "Model of Equatorial Scintillations From In-Situ Measurements," Radio Science, 11, 821-837.

Basu, Sunanda and Basu, Santimay, "Correlated Measurements of Scintillations and In-Situ F-Region Irregularities From OGO-6, Geophys. Res. Lett., 3, 681-684, 1976.

Fremouw, E. J. et al, "Early Results From The DNA Wideband Satellite Experiment-Complex-Signal Scintillation," Radio Science, 13, p. 167-187, 1978.

Vessot, R. F. C., and Levine, M. W., "A Preliminary Report On The Gravitational Red-Shift Rocket-Probe Experiment", Proc. International Symposium on Experimental Gravitation, Pavia, Italy, 17-20 September 1976.

Eshleman, V. R., Gallagher, D. B. and Barthle, R. C. (1960), "Radar Methods of Measuring The Cislunar Electron Density," J. G. R. Volume 65, pp 3079-3086. October

Burns, A. A., and Fremouw, E. J., (1970), "A Real-Time Correction Technique For Transionospheric Ranging Error," IEEE Transactions on Antenna and Propagation, Vol. AP-18, No. 6, pp 785-790, November.

4.0 PILOT BEAM SIZING & RFI

4.1 INTRODUCTION

The SPS power satellite requires a ground based pilot beam system to serve as a beacon for the retrodirective power beam. The pilot beam system employs a large Cassegrain reflector, a high power Klystron transmitter, and an angle tracking receiver. The communications link can use the same reflector via a dual frequency feed or dichroic subreflector. The pilot antenna is located in the center of the rectenna farm. Since the pilot system is a critical element in the system, a redundant pilot beam system should be provided. The pilot beam waveform consists of a pair of CW tones that are offset symmetrically in frequency from the frequency of the down-coming power beam. The frequency offset reduces the problem of receiving the pilot signal at a subarray in the presence of high power levels of the SPS array. The radiated pilot signal must be sufficiently strong so that it dominates all other in-band signals at the SPS subarrays including thermal noise. The signal should also have a clear spectrum with minimum harmonics and spurious components since it will be sidestepped in frequency and ultimately radiated as the power beam. If the pilot tones are not sufficiently stable (i.e., spread in bandwidth), it will cause phase reference errors across the array when the time delay across the array is comparable to the reciprocal of the bandwidth of the noise about the pilot tone. The high power pilot beam is a source of potential local interference and, hence, a Klystron tube having a state-of-the-art noise spectrum similar to that of the SPS Klystrons is assumed. The effects of ionospheric heating by the power beam on pilot beam propagation is of concern to SPS pointing safety due to the long leverage arm from the ionosphere to GEO.

4.2 PILOT BEAM SIZING

4.2.1 INTERFERENCE LEVELS

Figure 4-1 demonstrates that the received pilot signal (f_o + 100 MHz and f_o - 100 MHz) must be strong enough at an SPS subarray to overcome the following 3 sources of in-band interference: (1) thermal noise, (2) Klystron noise leakage

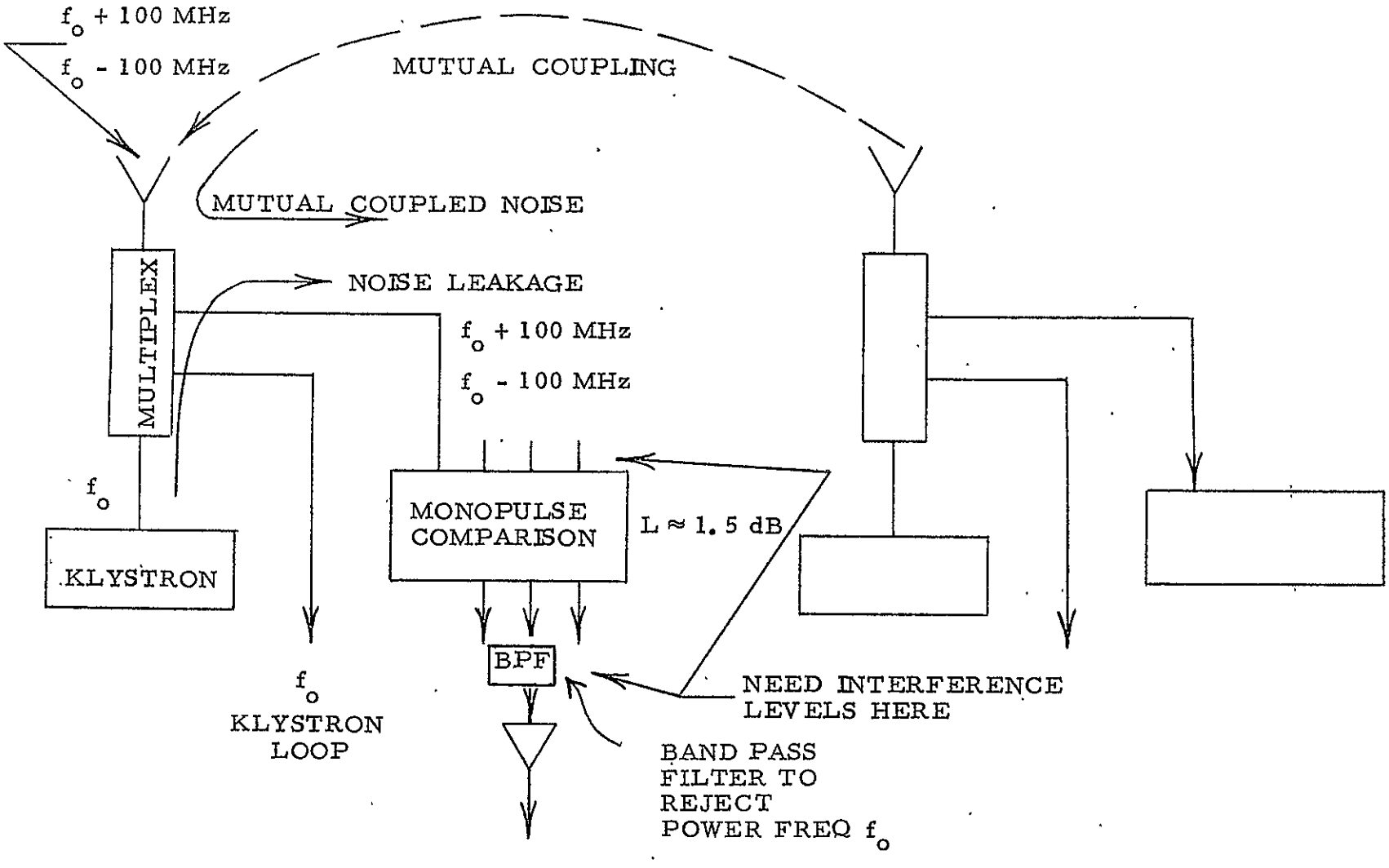

Figure 4-1. Interference Sources at SPS Subarray

through the diplexer, and (3) Klystron noise from other Klystrons through mutual coupling. Figure 4-1 also demonstrates that a filter is required to greatly attenuate the coupled carrier signal. Otherwise, leakage of the power signal might burn out or saturate the receiver. If the receiver is driven into the non-linear region, phase errors and intermods will be generated.

Table 4.1 shows a calculation of these 3 interference levels when the pilot tones are spaced by ±100 MHz and the bandwidth around each tone is 1 MHz. Diplexer leakage was estimated at 30 dB and mutual coupling was shown to be more than 40 dB down due to the large aperture size of each Klystron module radiator. Figure 4-2 shows the interference level for other pilot tone separations. If the separation is less than ±25 MHz, the major source of interference is coupled (interior or exterior to subarray) Klystron noise.

4.2.2 MUTUAL COUPLING

The Klystron noise is assumed to be uncorrelated from power module to power module, i.e., driver has good noise figure. The coupled Klystron noise is a random variable whose coupling is given by $\sum_{n=2}^{N} |\sin|^2$ where sin is the coupling between the power module of interest and the nth power module. Figure 4-3 summarizes the equations for calculating the coupling coefficients. The method is based on calculating the mutual admittance between apertures (i.e. power module cavity radiators) via an asymptotic expression and converting the admittance matrix to a scattering (i.e, mutual coupling) matrix. The resonant cavity resonator is modeled as a uniformly illuminated aperture that is matched to free space. Coupling was calculated for various power module sizes using a 49 element array of identical modules. The coupling varies somewhat with power module size but is typically about 50 dB for frequencies within 100 MHz of 2.45 GHz. A value of 40 dB was used in calculating interference levels to allow for some margin. Figure 4-4 lists the mutual coupling coefficients for a module size corresponding to 32 Klystrons/subarray. The self-term (reflection coefficient of -129.4 dB) shows that the modules are well matched in a passive environment. The coherent coupling at the carrier frequency of 2450 MHz is down 50.8 dB compared to the power delivered by the Klystron.

TABLE 4.1

PILOT TRANSMITTER SIZING

INTERFERENCE LEVELS

- RECEIVER THERMAL NOISE = $k\, t_o\, B\overline{NF}L$

$k = 1.38 \times 10^{-23}$ w-s/°k	=	-228.6 dBw
$t_o = 290°K$	=	24.6 dB
B = 1.0 MHz	=	60.0 dB
$\overline{NF}$	=	2.5 dB
L	=	1.5 dB
		-140.0 dBw = -110.0 dBm

- DIPLEXER LEAKAGE OF KLYSTRON NOISE AT PILOT FREQ

KLYSTRON CARRIER POWER, 50 KW	=	77.0 dBm
NOISE IN 1 MHz (PASSBAND)	=	-100.0 dBc/MHz
KLYSTRON ROLLOFF @ 100 MHz ΔF	=	-80.0 dB
DIPLEXER ISOLATION	=	-30.0 dB
		-133.0 dBm

- MUTUAL COUPLING NOISE FROM OTHER KLYSTRONS

KLYSTRON CARRIER, 50 KW	=	77.0 dBm
NOISE IN 1 MHz	=	-100.0 dB
KLYSTRON ROLLOFF @ ΔF = 100 MHz	=	-80.0 dB
MUTUAL COUPLING	=	-40.0 dB
		-143.0 dBm

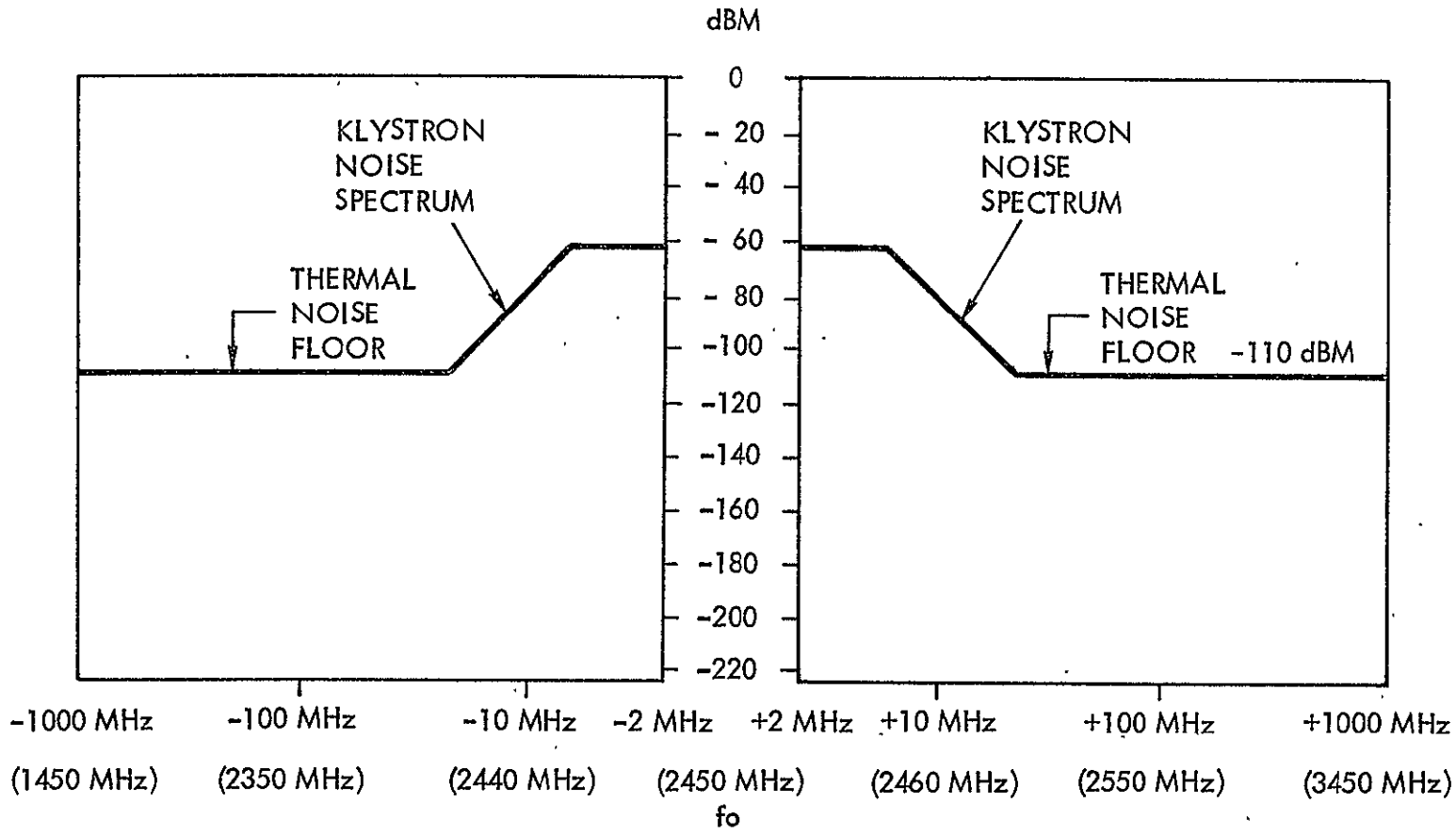

Figure 4-2. Total Interference vs Pilot Beam Frequency

MUTUAL ADMITTANCE:

$$Y(S) = \frac{1}{k\,120\pi} \iint_{-\infty}^{\infty} \frac{k^2\,\epsilon\rho(u)\,\epsilon\rho(-u) + W^2\,\epsilon\psi(u)\,\epsilon\psi(-u)}{W}\, e^{-jus}\, du$$

$$S = (\Delta x, \Delta y)$$

$$u = (\sin\alpha, \sin\beta) = (u, v)$$

$$W = \sqrt{k^2 - u^2 - v^2} \quad , \quad u^2 + v^2 \le k^2$$

$$-j\sqrt{u^2 + v^2 - k^2} \quad , \quad u^2 + v^2 \ge k^2$$

ASYMPTOTIC EVALUATION:

$$Y_E(S) = j\,\frac{2\pi k\, e^{-jk|S|}}{120\pi\,|S|}\, |\epsilon\rho(k\cos\phi, k\sin\phi)|^2$$

$$Y_H(S) = \frac{4\pi}{120\pi\,|S|^2}\, e^{-jk|S|}\, |\epsilon\psi(k\cos\phi, k\sin\phi)|^2$$

$$\epsilon\rho = \epsilon_x \cos\psi + \epsilon_y \sin\psi$$

$$\epsilon\psi = \epsilon_x \sin\psi + \epsilon_y \cos\psi$$

$$[S] = [Y_g I - Y]\,[Y_g I + Y]^{-1}$$

$$Y_g = \frac{1}{120\pi}$$

$$\epsilon_x = 0$$

$$\epsilon_y = \frac{\sqrt{ab}}{2\pi}\, \frac{\sin(kV\, b/2)}{(kv\, b/2)}\, \frac{\sin(ku\, a/2)}{(ku\, a/2)}$$

Figure 4-3. Mutual Coupling Calculations

POWER MODULE AMP. TAPER:
HORIZONTAL - UNIFORM
VERTICAL - UNIFORM

-126.3dB (-57.8°)	-136.1 (97.2)	-122.3 (30.5)	-77.1 (-42.7)	-122.3 (30.5)	-136.1 (97.2)	
-142.2 (71.4)	-123.6 (-47.5)	-124.3 (-16.3)	-70.1 (31.5)			
-91.3 (-100.6)	-108.2 (139.9)	-116.8 (22.5)	-58.0 (105.8)			
-71.0 (36.8)	-67.5 (-5.5°)	-61.4 (-47.7)	-108.6 -129.4			
-71.3 (-100.6)						

NON-COHERENT
POWER COUPLING - 52.7 dB

COHERENT
COUPLING - 50.8 dB $\angle 30.7°$

Figure 4-4. Coupling Coefficients

4.2.3 SUPPRESSION OF KLYSTRON LEAKAGE

The Klystron amplifier has an output of 50 KW (77 dBm) at 2.45 GHz and the duplexer isolation is typically 30 dB. Hence, the carrier to noise ratio is 157 dB at the receiver (i. e, greatly exceeding the receiver's 75 dB dynamic range). Figure 4-5 shows the filtering capability of multi-pole Chrebyshev filters. Increasing the number of poles improves the rejection of the Klystron carrier at the expense of loss in the past band of the pilot tone. The loss, however, is quite low and can be compensated for by a slightly larger pilot transmitter. The filter can be located in the sum and difference output ports of the subarray's monopulse stripline comparator.

4.2.4 PILOT BEAM TRANSMITTER POWER

The pilot beam transmitter must be large enough so that the signal received at a subarray is greater than any other interference such as thermal noise and coupled Klystron noise. Figure 4-6 shows that the contribution to phase error by noisy interference is 1.8° RMS when the pilot is sized to produce a 30 dB signal-to-interference ratio at each subarray. The power scattered from the power beam due to these subarray-to-subarray uncorrelated errors is about 8 MW (i. e., 0.1%). When the pilot tones are separated by ±100 MHz, the required pilot level at the subarray is -80 dBm. Figure 4-6 shows that this corresponds to a pilot ERP of 35 dB if the entire subarray is used to receive the signal. If only a central Klystron module is used the pilot ERP must be 49 dB. These pilot requirements are easily satisfied by a 10m antenna and a 100 watt transmitter. Figure 4-6 shows that the transmitter size grows quite rapidly due to the increased level of Klystron noise coupling as shown in Figure 4-2. Rejection of the coupled carrier is more difficult and may require adaptive feed-through nulling as used in CW radars such as Hawk and Seasparrow tracking illuminators. If the pilot tone separation is within ± 5MHz, a 45 KW pilot transmitter is required with a 10 m reflector.

4.3 SPS RFI PROBLEMS

4.3.1 SPS NOISE LEVELS ON THE EARTH'S SURFACE (SINGLE SPS)

The ultra high powered SPS radiation with its associated noise and harmonics is a potential source of RFI. Sensitive satellite and earth-based

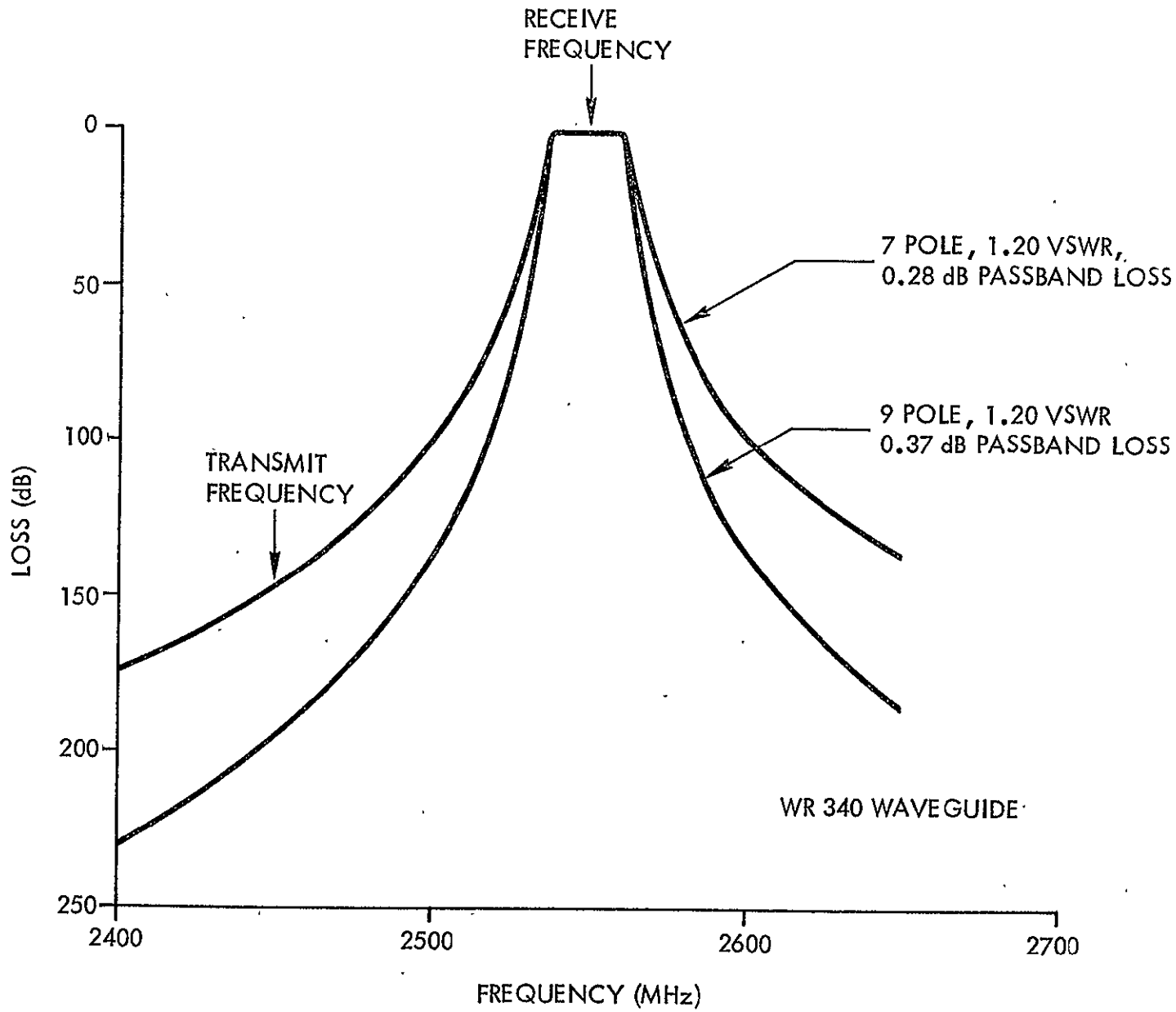

Figure 4-5. Cancellation of Transmit Leakage Using a Chebyschev Filter

S/I	$\sigma\phi$	LOSS IN POWER	POWER LOST (XMIT 7.36 GW)	COST TO SYSTEM TO REPLACE
30 dB	1.8°	0.1%	8.07 MW	$1.9M
40 dB	0.6°	0.01%	807 KW	$186K

Based on JSC SPS production cost of $22.9B/ 10 GW = $230/KW

$S/I = 30\ dB \Rightarrow S = -80\ dBm = -110\ dBw = 10^{-11}$ WATTS

$$\frac{P_T G_T A}{4\pi R^2} = 10^{-11} \quad \text{WHERE } R = 3.8 \times 10^7 m \ \& \ A = 0.5\,(10.2m)\,(11.64m) = 59.4m^2$$

USE FULL SUBARRAY

$P_T G_T = 3.054 \times 10^3$

$G_T = \eta \left(\frac{\pi D}{\lambda}\right)^2 =$ 45.4 dB FOR $D = 10m$, $\lambda = 0.12m$, $\eta = 50\%$

$\therefore P_T = 0.089$ WATTS @ $\Delta F = 100$ MHz

P_T & G_T vs. ΔF (10.2m x 11.64m SUBARRAY)

ΔF (MHz)	Antenna Dia. m	G_T (dB)	P_T^*
1	10	45.4	44.6 KW
1	30	54.9	5.0 KW
5	10	45.4	44.6 KW
5	30	54.9	5.0 KW
10	10	45.4	141 W
30	10	45.4	0.1 W
100	10	45.4	0.1 W

Thermal Noise Limited

*$P_T \approx 25$ times greater if 1/50 subarray used (central Klystron module) and aperture $\eta \sim 100\%$.

Figure 4-6. Pilot Transmitter Sizing

receivers could be susceptible to sidelobe radiation or scattering of the main beam by rain or clouds. Harmonics generated by the rectenna elements might be a local problem. Systems affected most will be sensitive receivers aimed toward the SPS; i. e., satellite communications, radio astronomy, deep space research, surface microwave links, radars, etc. In order to assess the interference, one must compute the power density over the earth as a function of frequency. Figure 4-7 shows the power density on the earth of the near-in noise (± 5 MHz from carrier) for a single SPS. This level would increase the noise level by 34 dB in a radio astronomy system having a 0.2 dB noise figure and a 10m diameter reflector that was pointed toward the SPS. Multiple SPS systems would raise the level by the number of systems expressed in dB. In order to plot the power density as a function of frequency, one must know the Klystron noise spectrum and filtering by the resonant cavity radiators. Varian states that the SPS Klystron passband noise level is -100 dBc/MHz PM and -110 dBc/MHz AM. This is quite reasonable since a 35 dB NF, 50 KW tube with 50 dB gain has a theoretical passband noise level of -106 dBc/MHz. This assumes that the driver has a better noise figure than the tube. The noise spectrum of the Klystron is defined as follows. The close-in noise follows the gain characteristic of the tube down to unity gain (i. e., 30 dB/octave roll-off for 5 cavity Klystron). Below unity gain, the noise rolls off with only the filtering of the output cavity (i. e., 6 dB/octaves). The slotted array is a resonant structure having a high Q that provides additional filtering. The waveguide cutoff provides severe attentuation at the lower frequencies. Figure 4-8 shows the power density on the earth as a function of frequency. Figure 4-9 shows that the harmonic level of Klystrons is typically 70 dB down from the carrier. The power level on the earth depends upon the subarray-to-subarray correlation at the harmonic frequency. If the Klystrons are uncorrelated, the SPS average gain at the harmonic is simply the gain of a typical Klystron module radiator.

4.3.2 POWER DENSITY FROM THE PILOT BEAM

Interference from the pilot system sidelobes is a local phenomena. Figure 4-10 shows the power density at a distance of 10 Km from the pilot transmitter as a function of pilot tone separation (i. e., pilot transmitter power to maintain 30 dB S/I at satellite).

$$P_D = \frac{N\, P_T\, G_{SA}\, C}{4\pi R^2}$$

	dB
$N = 1$	0.0 dB
$P_T = 7.362$ GW	98.7 dBW
4π	-11.0 dB
R^2 $(3.8 \times 10^7 m)$	-151.6 dB
G_{SA}	36.9 dBi
C (-160 dBc/Hz)	-160.0 dBc/Hz
	-187.0 dBW/m^2 Hz

CLOSE-IN NOISE LEVEL

Figure 4-7. Noise on Earth From SPS Array

NO. SPS SYSTEMS	NOISE LEVEL INCREASE (dB)
1	0
30	14.8
60	17.8
120	20.8

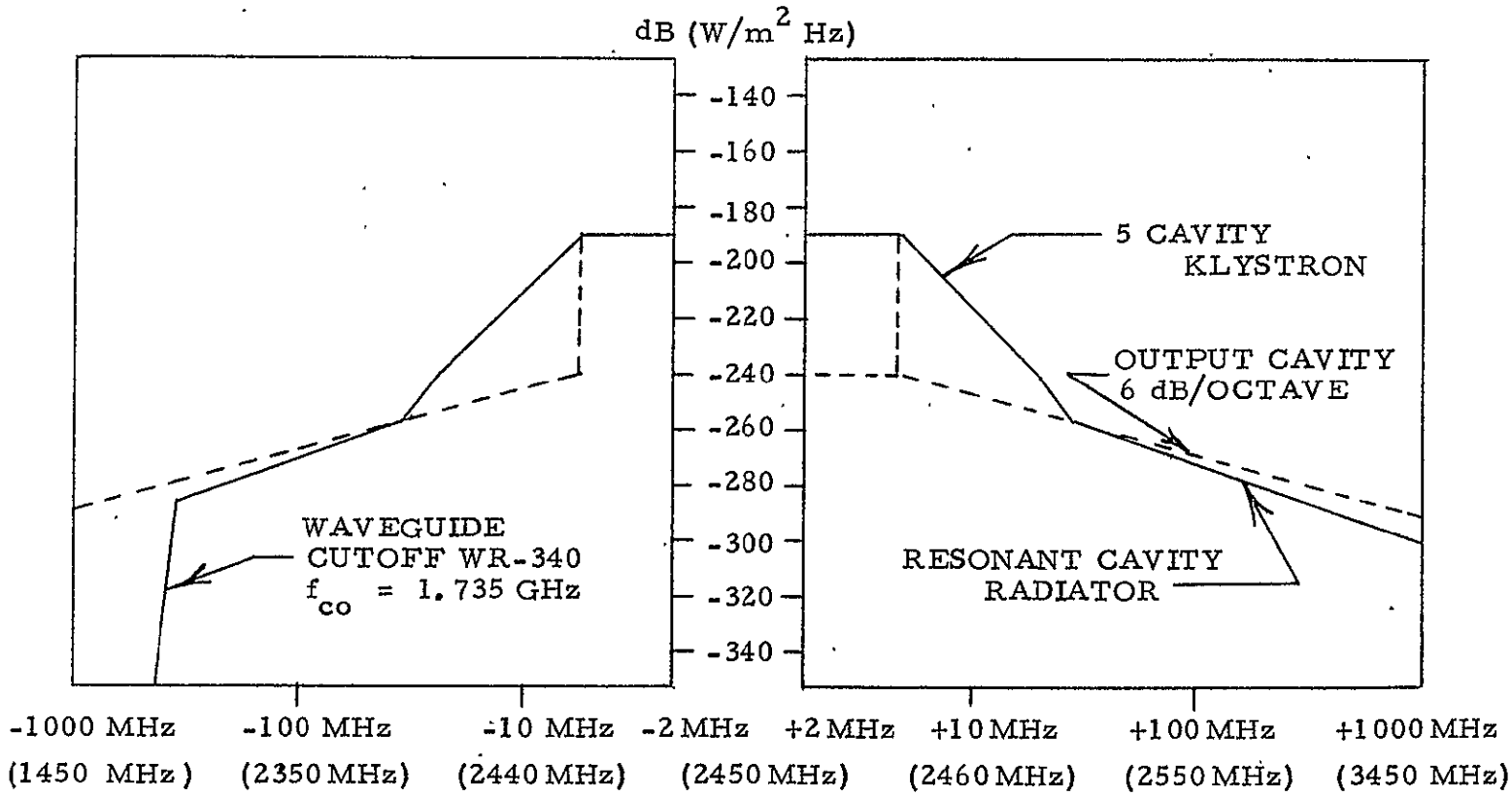

Figure 4-8. SPS Noise Level at Earth (Single SPS)

Harmonic / Converter	2	3	4	5	6	7	8
Magnetron:							
Mean	78.1	71.7	77.7	86	87.2	91.9	99.3
Range	57/103	45/100	62/93	67/114	76/96	81/96	83/114
Samples	77	59	34	23	17	7	5
Klystron:							
Mean	71.3	78.2	76.9	73.9	82.3	87.2	
Range	38/119	57/105	56/101	59/111	73/89	72/97	
Samples	44	27	21	8	7	4	

Figure 4-9. Harmonic Output of Converters in dB Below Fundamental
(Radar Handbook, Skolnik, p. 29-G)

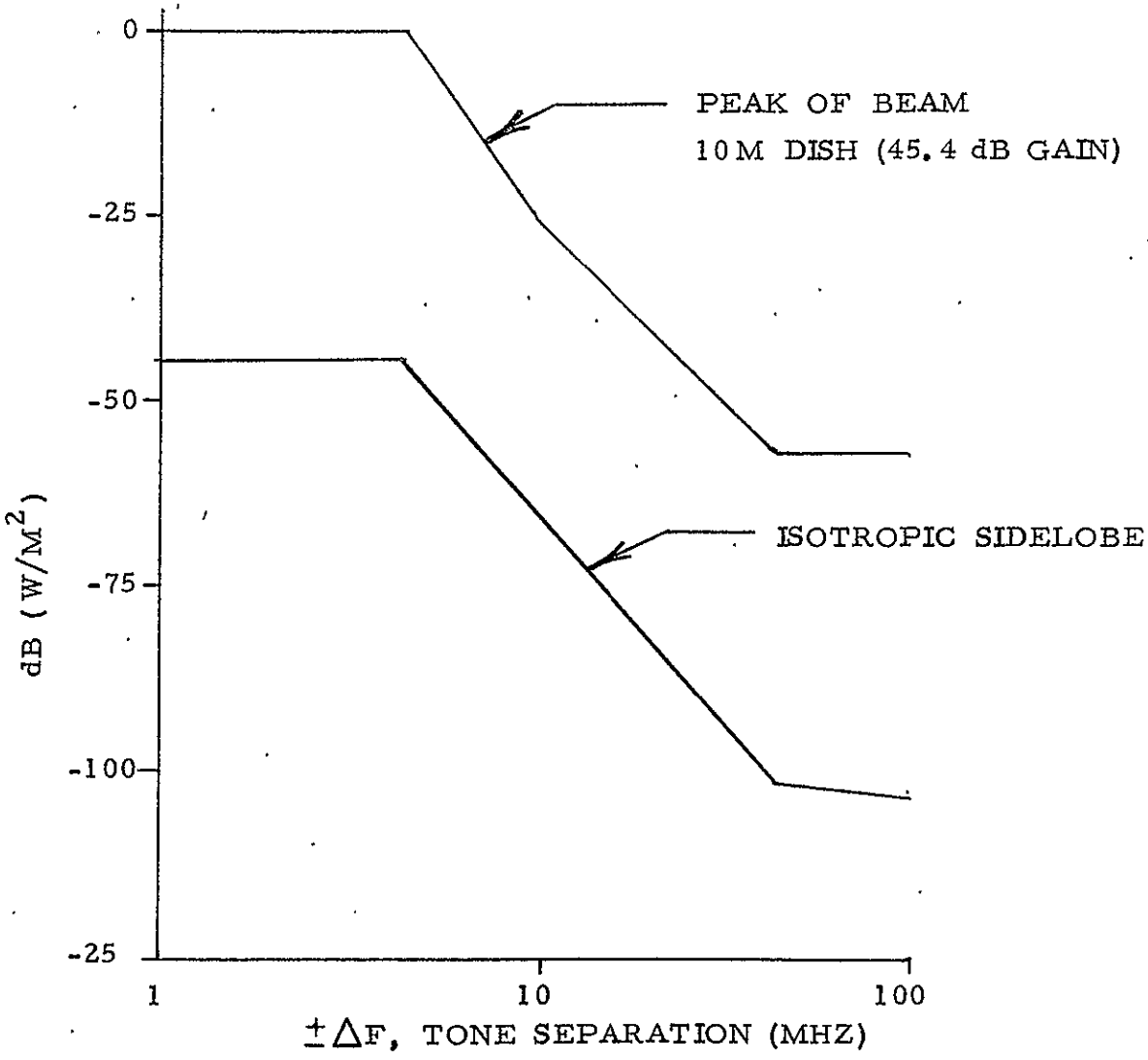

Figure 4-10. Power Density in Vicinity of Pilot Transmitter (Range = 10 KM)

Multiple pilot transmitters on the earth create an interference problem at a given SPS system. Only one pilot beam is actually aimed at that SPS but the sidelobes of the other pilot beams are an interference source. Figure 4-11 shows that 100 SPS systems can be spread over a 60° equatorial arc with only one SPS in a given pilot beam. If the pilot beam peak sidelobes are less than 20 dB, all the interference pilot beams cannot create as much power at a particular SPS as its dedicated pilot beam.

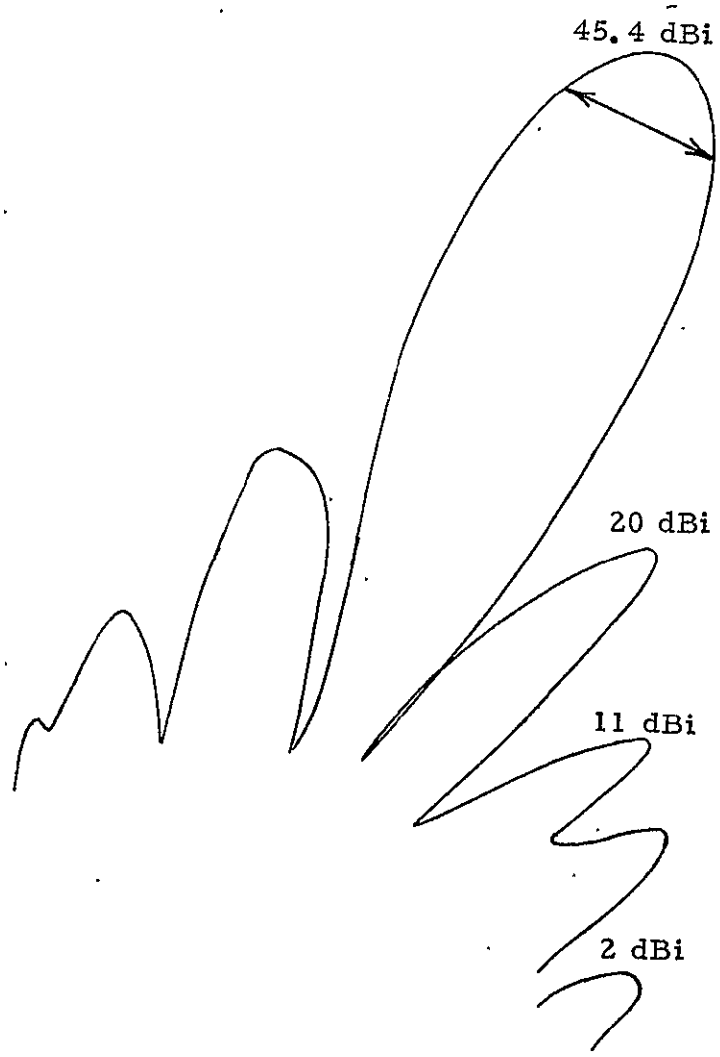

SIDELOBES DELAY AS $1/x^{3/2}$

9 dB/OCTAVE

$\theta_3 \approx 0.73°$.

3.8×10^5 M AT 3.8×10^7 M

SPS SPREAD OVER 60° IMPLIES

$$\Delta \sim \frac{2\pi (3.8 \times 10^7)}{6} \sim 3.8 \times 10^7$$

APPROXIMATELY ONE IN MAIN BEAM

Figure 4-11. RFI in Orbit due to Multiple Pilot Transmitters

5.0 COMMUNICATIONS SUBSYSTEM

5.1 INTRODUCTION

This task is to define and assess the communications systems associated with the SPS as an operational space station. The sizing of the system (its power aperture product) is the most important parameter to be investigated, the RFI characteristics are to be evaluated and message security must be considered.

The evaluation of the baseline data led to subdividing the requirements into four categories:

1. Command and Control
2. Telemetry
3. Operations
4. Entertainment

5.2 COMMUNICATION REQUIREMENTS

5.2.1 TELEMETRY (SPS TO GROUND)

The details of a telemetry system will define requirements for the SPS power beam transmitter segment as the prime source of information to be transferred to earth. The key element of the SPS power beam is the amplifier chain. The update cycle for this data is arbitrary but once a per shift (8 hours) is a reasonable rate. Given up to 10^6 transmitter tubes, phase shifters, etc. and 64 bits to describe each element, the information transfer need in bits/sec is $10^6 \times 64 \div 8 \div 3600 = 2.22$ kb/sec. If about 10% is added to this to provide framing to identify the data elements, it is seen that a 2400 b/s data stream is required.

It is estimated that the reports for the power generation system can be handled by a similar transmission capacity.

There will be other requirements such as reports on the star tracker system and the reports on the medical status of each crewman that are to be met. The positioning data can be monitored with a 600 b/s facility and medical data on each crewman can be carried with less than 4800 b/s. The medical report assumes that two crewmen are undergoing special treatment and that EKG, blood pressure, pulse, etc. are to be monitored on a full time basis.

The telemetry needs are summarized as:

Tube Data at 64 bits/tube/8 hrs.	2.4 kb/s
Power System Data	2.4 kb/s
Positioning Data	0.6 kb/s
Medical	< 4.8 kb/s
TOTAL	9.6 kb/s

5.2.2 COMMAND AND CONTROL (GROUND TO SPS)

A key segment of a command control link is the need for any emergency messages. For SPS the key command in this sense is to power down the RF beam. The average data flow for needs of this nature are negligible and cannot be sized on an average basis. Provision for this transmission is to be integrated into the overall system.

The SPS power beam will impinge upon the rectenna and sensors will evaluate the positioning of the beam as well as the power density. This data will be provided to the rectenna control station, the master control station(s), and the satellite. A transmission rate of 100 b/s will allow all stations to be informed.

Related to positional data is a potential need to command the phase shifters from the ground. This would be as a backup to the retrodirective control system. To estimate this, it was assumed that 10^6 phase shifters were to be controlled and that a complete update was made every 20 seconds. If an 8 bit command is sent, then a 400 kb/s channel is needed. The identification of the phase shifter or addressing can be covered by another 100 kb/s.

The command and control link is the counterpart to telemetry in that this data flow is earth to satellite.

5.2.3 OPERATIONS (TWO-WAY LINK)

The tasks performed for each shift will require both voice and data transmissions. The technical crew on duty will handle administrative as well as real time traffic.

The size of the duty crew was estimated at 9 and their voice needs could be handled by 4 channels. This may or may not mean party line installations. Four telephone channels with pulse code modulation using the standard 64 kb/s per channel require a 256 kb/s transmission circuit.

The voice traffic is one facet of human to human communications. The other is termed record data or message data. There will be a need to exchange written instructions and reports. In this case the cathode ray tube display will probably replace paper and the computer memory will enable storage and recall of records. The crew will send and receive personal communications from family and friends via this channel. A channel of 9.6 kb/s will transfer two pages of text every second. This rate exceeds the average need but is chosen to provide a system whose transmission time is small compared to the reading time.

A similar channel of 9.6 kb/s is established for the computer to computer information exchange. The detailed requirement has not been synthesized but based on the record data channel it is considered appropriate.

During the period when a supply spacecraft is en route, there could be a need for a voice and data circuit. The voice is again 64 kb/s and the data 9.6 kb/s.

OPERATIONS

VOICE (4 CHANNELS AT 64 KB/S)	256 KB/S
RECORD DATA	9.6 KB/S
COMPUTER TO COMPUTER	9.6 KB/S
SPACECRAFT TO SHUTTLE	
1 VOICE	64 KB/S
1 DATA	9.6 KB/S

5.2.4 ENTERTAINMENT

The need for an entertainment system stems from the crew that will be resident on the SPS. The size of the crew is assumed to be 50 persons and they are divided into technical and support categories. For a total crew of 50, it is estimated that 14 will be required for the hotel and medical teams leaving 36 for the technical crew. Four technical crews can cover the station requirement 24 hours each day with each crew working 42 hours per week on the average.

Unlike a vessel in the ocean, the SPS is able to receive television programs and need not carry a store of motion picture films for visual entertainment. Two approaches can be taken. First, two TV signals could be sent to the SPS with the ability to select from available networks the channels to be transmitted or to design a four channel transmission which allows the personnel to select the program. The design of the living spaces will determine the better of these approaches.

5.3 COMMUNICATION SUMMARY

5.3.1 DIGITAL COMMUNICATIONS SUMMARY

The summary of the data rate requires are:

Telemetry	9.6 kb/s
Operations	
Voice (5 x 64 kb/s)	320.0 kb/s
Data (3 x 9.6 kb/s)	28.8 kb/s
Command and Control	500.0 kb/s

This digital traffic should be multiplexed onto a single serial data bit stream. The standard T1 transmission rate and related multiplexers should meet this need.

The multiplexer accepts voice signals and converts each to 64 kb/s of digital information. There are 24 channels in the multiplexer and, if data is transmitted rather than voice, there is the potential for a 56 kb/s data throughput per channel. This would mean that the multiplexer assignment could be set up as shown below.

To SPS	Channel	From SPS
Voice	1 through 5	Voice
Command & Control	6 through 15	Unused
Record Data, Computer Data, Shuttle Data	16	Same
Unused	17 through 24	Unused

The T1 rate of 1.544 Mb/s is standard in many telephone applications. This means that a standard transmission could be used to transfer information from the earth terminal to other mission control centers.

There are standard encryption equipments that can be used with T1 rate systems that will provide a transmission security. End to end security does not appear to be a requirement which simplifies installation and local distribution.

5.3.2 ENTERTAINMENT TRANSMISSION SYSTEM

The bandwidth requirements for a television signal require a 40 MHz channel. When this is compared with the 1.5 MHz or 3.0 MHz channel requirement for the data traffic, it is obvious that the entertainment system will drive this design of the radio equipment design.

5.3.3 TRANSMITTED POWER REQUIRED

A calculation of the required transmitter power showed that 25 mW equipment would satisfy the need for the 1.544 Mb/s voice plus data levels. For 60 SPS system combined into a single 60 group return, a transmitter power of 1.7 W would be required. The color TV links for each SPS would require 1 Watt.

These calculations assumed:

1. 8 GHz Grequency Band
2. 20 Meter Gound Antenna
3. 3 Meter Spacecraft Antenna
4. 8 dB System Noise Factor

5.4 FREQUENCY ALLOCATION AND RFI

The channel assignments for a communication system for SPS will probably fall within the government bands. This could be true whether the services are supplied by a government communication service or supplied by a common carrier. There is the possibility that if the services are supplied by a common carrier that a common carrier band may be employed.

At this time, the majority of the government band communications services via satellite employ the 7 - 8 GHz band. There is some work at 14 GHz, 30 GHz, and 40 GHz. The selection is not too important.

If the antenna size were critical, then the 14 GHz band might be desired. The rain margin can be small and the net system loss is less if the antenna size is fixed.

The RFI created by the communication system will be small. Most terminals employ transmitters with kilowatts of average power. Thus coordination of frequency assignments with other stations should not be difficult. The RFI from the power beam is not expected to be significant. The broadband noise in the bands of interest will be very low in power. The harmonics of 2.45 GHz cannot be neglected but do not fall into the bands of interest. The potential exception is the space-earth link which could be in the band 7250 - 7750 MHz which includes the third harmonic of 2450 MHz or 7350 MHz.

A detailed study relative to the location of the antenna on earth and the harmonic levels to be experienced could quantify this problem. However, it will not be a deterrent to the SPS program because locations can be found for this system that will withstand the environment created by SPS. The basis for further study will be these data from the power beam RFI study and work should be delayed until results are available.

5.5 RECOMMENDATIONS FOR PHASE II

The communication requirements and resultant sizing of the Communication system have been provided. The study has demonstrated that the SPS communication requirements are relatively modest and will not create a significant RFI problem. There remains, however, the question of how to distribute the

information to the space stations. Figure 5.1 shows a simple network. The Central Control talks directly to the Rectenna Control station and the Rectenna station talks to the SPS. This is a form of "corporate" structure communications. A centralized network is a possibility and leads to an interesting antenna complex if all earth-space links terminate at a central site. Phased array and multibeam array concepts can be explored as a means to lower costs. In this same vein, sharing the pilot beam antenna is a possibility that could be the lowest cost approach.

As a result of this study, we recommend that during the Phase II program the issue of centralized bs decentralized communication network be explored. However, as we feel that this is a low priority effort and could, without impacting on the SPS development (at least as we view it), be delayed to a later time.

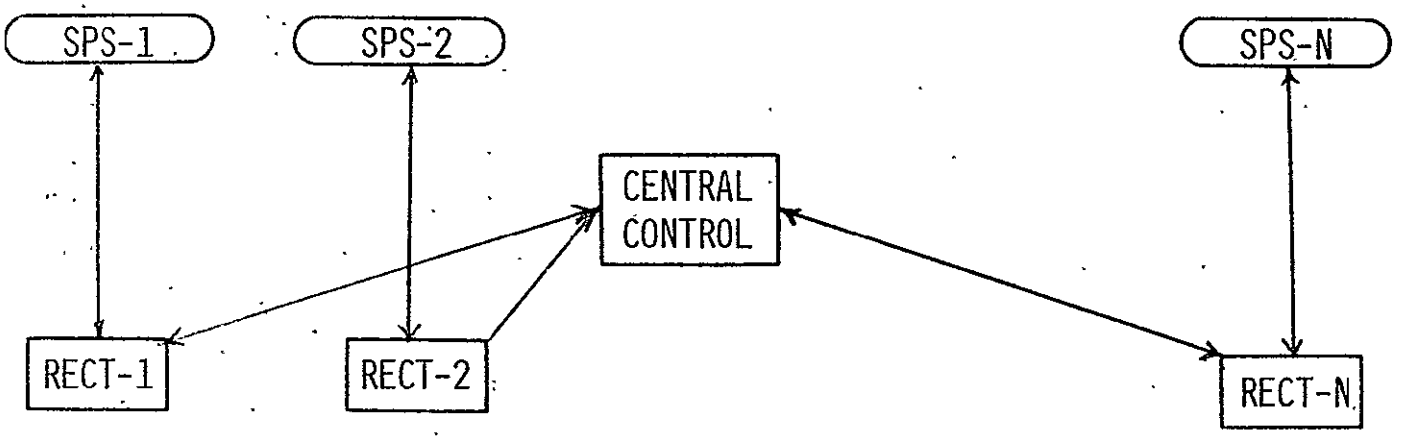

- DECENTRALIZED
- CENTRALIZED
- INTERRATED WITH ANTENNA FOR PILOT BEAM

Figure 5.1. Communications System Network